ACSNANO

www.acsnano.org

REVIEW

Single-Molecule Junction: A Reliable Platform for Monitoring Molecular Physical and Chemical Processes

Xinmiao Xie,[§] Peihui Li,[§] Yanxia Xu, Li Zhou, Yong Yan, Linghai Xie,* Chuancheng Jia,* and Xuefeng Guo*

Cite This: https://doi.org/10.1021/acsnano.1c11433

Read Online

ACCESS | Metrics & More | Article Recommendations

ABSTRACT: Monitoring and manipulating the physical and chemical behavior of single molecules is an important development direction of molecular electronics that aids in understanding the molecular world at the single-molecule level. The electrical detection platform based on single-molecule junctions can monitor physical and chemical processes at the single-molecule level with a high temporal resolution, stability, and signal-to-noise ratio. Recently, the combination of single-molecule junctions with different multimodal control systems has been widely used to explore significant physical and chemical phenomena because of its powerful monitoring and control capabilities. In this review, we focus on the applications of single-molecule junctions in monitoring molecular physical and chemical processes. The methods developed for characterizing single-molecule charge transfer and spin characteristics as well as revealing the corresponding intrinsic mechanisms are introduced. Dynamic detection and regulation of single-molecule conformational isomerization, intermolecular interactions, and chemical reactions are also discussed in detail. In addition to these dynamic investigations, this review discusses the open challenges of single-molecule detection in the fields of physics and chemistry and proposes some potential applications in this field.

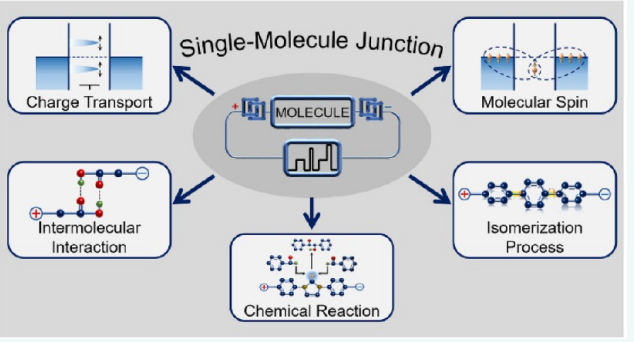

KEYWORDS: *in situ monitoring, single-molecule junction, molecular electronics, charge transport, spin characteristics, conformational isomerization, intermolecular interaction, chemical reaction*

Single-molecule science is concerned with the physical and chemical properties of individual small molecules, atomic clusters, and biomolecules as well as their interactions with the external environment. The study of single-molecule systems has many important scientific significances.[1−3] First, single-molecule technology can explore fundamental physical and chemical effects at the single-molecule level. For instance, quantum behavior determines the main properties of a system because of the ultrasmall size at the single-molecule level, which often leads to different characteristics from the macroscopic system. Second, measuring many molecular aggregates only gives an overall average result, whereas measuring a single molecule excludes this average effect. Third, it can effectively monitor the time-dependent changes of physical and chemical processes, which aids in understanding the dynamic changes at the single-molecule level. Because of these advantages, single-molecule sciences have become a frontier interdisciplinary subject, which provides a powerful platform for exploring basic physical and chemical principles.[4−9] For example, the process of several meaningful physical effects, such as Coulomb blockade,[10,11] Kondo effect,[12−15] spin-crossover effect,[16−18] stereoelectronic effect,[19,20] and isomerization effect, has been fully explored at the single-molecule level.[21,22] Simultaneously, monitoring chemical reaction processes has also reached the single-molecule level, such as exploring nucleophilic substitution,[23] nucleophilic addition,[24] Diels−Alder reactions,[25,26] as well as Suzuki−Miyaura coupling reaction.[27]

Received: December 23, 2021
Accepted: February 14, 2022

Table 1. Comparison of Single-Molecule Junctions Fabricated by Different Approaches

Single-molecule junctions	Schematics	Advantages	Ref.
Scanning tunnelling microscopy break junction	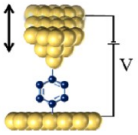	Repeatability Convenient preparation	100
Mechanically controllable break junction	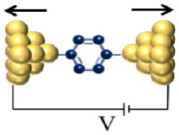	Repeatability Precise control	164
Atomic force microscopy break junction	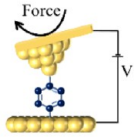	Repeatability Information for mechanics	108
Electromigration break junction	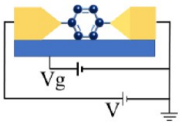	Device configuration Fine compatibility	70
Carbon nanotube-based junction	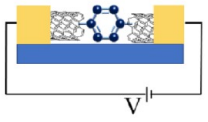	High stability Size matching	90
Graphene-based junction	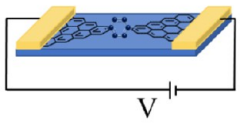	High stability High success rate	27

Table 2. Comparison of Molecule-Electrode Connections[a]

Covalent bonds	Donor–acceptor bonds		Electrostatic interaction
	Lone pair system	π–conjugation system	
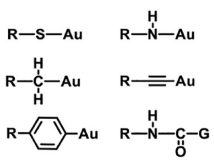	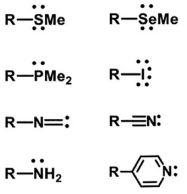	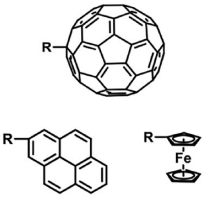	

[a]Abbreviations: R, core molecule; G, graphene.

Nowadays, several single-molecule techniques have been developed. Different physical and chemical processes of single molecules can be detected using optical, force, and electrical signals.[28] For instance, super-resolution fluorescence microscopy,[29] scanning near-field optical microscopy (SNOM),[30] and surface plasmon resonance enhancement[31] can monitor single-molecule information using optical signals. Techniques such as atomic force microscopy (AFM), optical tweezer, and magnetic tweezer can detect single-molecule information through force control.[32,33] The electrical techniques used for monitoring single-molecule behaviors include scanning probe microscope, single-molecule junctions, field-effect transistors based on nanowire or nanotube, nanopore technology, and other electrical techniques.[34−37] Among them, the electrical single-molecule junction platform uses a single molecule as a conductive channel to directly convert the changed molecular states into resolvable electronic signals.[38−40] Therefore, single-molecule junctions can be used for real-time monitoring of molecular physical and chemical processes. Single-molecule junction techniques include mechanically controllable break junctions (MCBJs), scanning tunneling microscopy break junctions (STM-BJ), conductive AFM junctions, electromigration junctions, graphene−molecule−graphene single-molecule junctions (GMG-SMJs), and others.[41−44] Moreover, the success of the connection of target molecules can also be characterized by a variety of detection methods, such as IETS[45,46] and AFM.[47,48] In addition, the recently developed optical and electrical synchronous detection technology also

https://doi.org/10.1021/acsnano.1c11433
ACS Nano XXXX, XXX, XXX−XXX

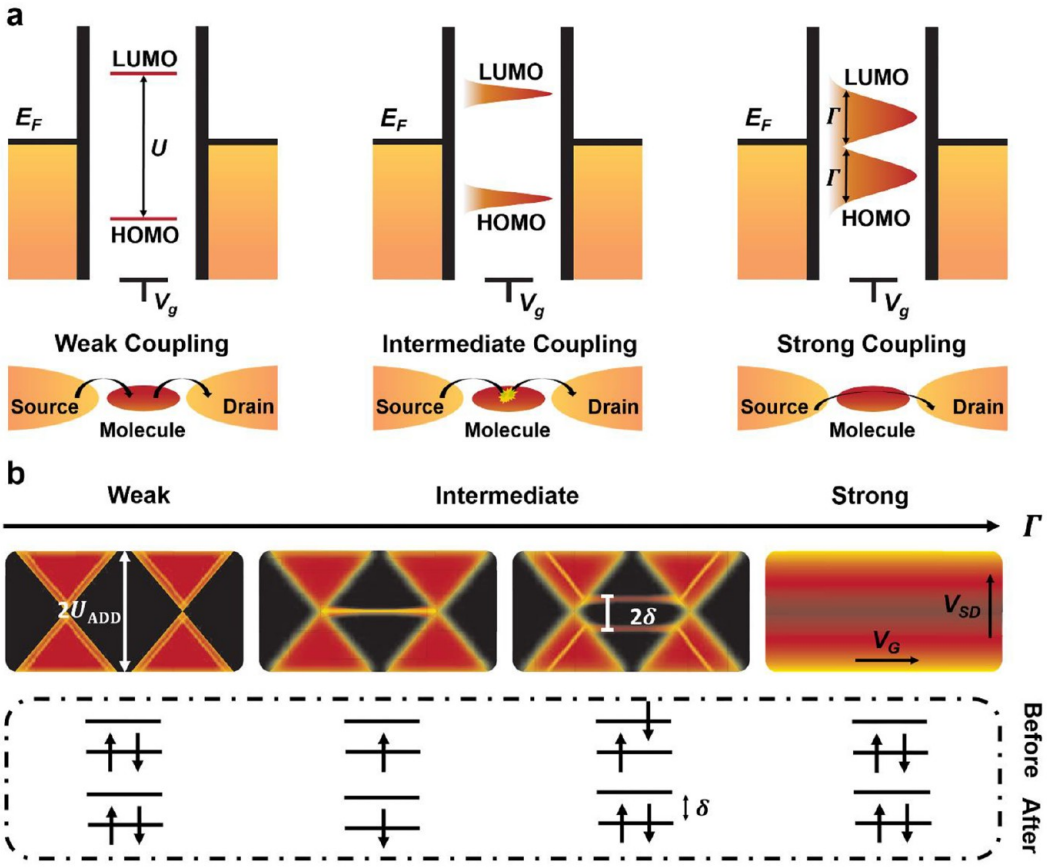

Figure 1. (a) Schematic representation of the energy levels and charge transport processes through single molecules with different coupling strengths between the molecules and the electrodes. Reprinted with permission from ref 49. Copyright 2013 Royal Society of Chemistry. (b) Electron transport at different coupling strengths in a three-terminal device. Reprinted with permission from ref 50. Copyright 2009 Springer Nature.

strongly demonstrates the reliability of single-molecule junctions.[26,27] These single-molecule junctions can be used to detect the corresponding physical or chemical states of single molecules by monitoring their charge transport. Therefore, single-molecule junctions enable the discovery of fundamental physical and chemical phenomena at the single-molecule level. Various fabrication strategies for single-molecule junctions are summarized in Table 1. In addition, different molecular terminal groups and the corresponding connection modes are also provided in Table 2.

This study introduces the applications of single-molecule junctions in physical and chemical behavior monitoring and provides insights into the latest developments in this field. First, gating methods for regulating the charge transport process of single molecules are introduced, including solid and liquid gates. Additionally, research on monitoring the spin characteristics of single molecules, such as the Kondo effect, Zeeman splitting, and spin crossover, is discussed. After that, the monitoring of molecular conformational isomerization, intermolecular interactions, and chemical reactions using single-molecule devices is discussed in detail. Finally, the challenges faced by single-molecule devices in monitoring physical or chemical processes are discussed, and solutions to overcome current obstacles are proposed.

MONITORING OF CHARGE TRANSPORT OF SINGLE MOLECULES

Monitoring charge transport aids in understanding the basic laws of the complex charge transport process in single-molecule devices, which regulate the process accurately. Starting with the basic physical characteristics of charge transport through single molecules, this section introduces the inherent mechanism of gate regulation of charge transport and different types of gate regulation methods.

Key Factors of Charge Transport through Single Molecules. Two critical factors influencing the process of charge transport through single molecules that can be monitored by single-molecule devices include electronic coupling of the molecule−electrode interface and relative energy-level position.[49,50] The coupling strength between electrons in the molecules and those in the electrodes can cause different charge transport behavior in single-molecule devices. The coupling strength is accurately defined by comparing the coupling parameter (Γ) and addition energy (U). The former (Γ) is the broadening of the molecular energy levels due to the coupling between the molecules and electrodes. The latter (U) is the energy difference of taking one electron from the highest occupied molecular orbital (HOMO) of the system and injecting one electron to the lowest unoccupied molecular orbital (LUMO). When $\Gamma \ll U$, the system is in the weak coupling regime, whereas for $\Gamma \gg U$, the system is in the strong coupling regime (Figure 1a).

https://doi.org/10.1021/acsnano.1c11433
ACS Nano XXXX, XXX, XXX−XXX

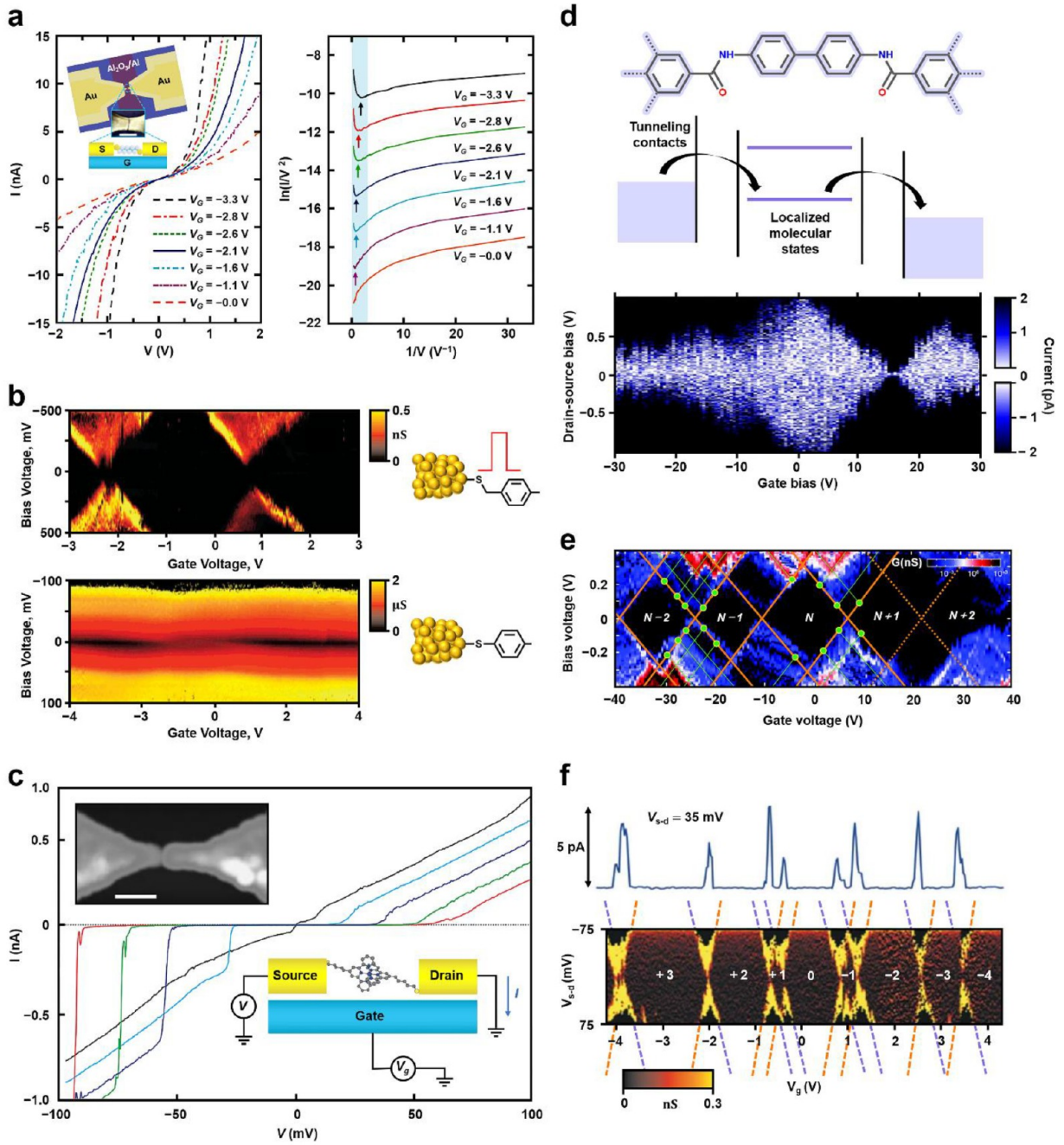

Figure 2. (a) Representative $I-V$ curves measured at 4.2 K for different values of V_g. Inset: The device structure and schematic. Reprinted with permission from ref 51. Copyright 2009 Springer Nature. (b) Comparison of electron transport characteristics of OPV3 molecules with different coupling strengths. Reprinted with permission from ref 52. Copyright 2008 American Chemical Society. (c) Representative $I-V$ curves measured for different values of V_g in a single-electron transistor. Upper inset: A topographic atomic force microscope image of the electrodes with a gap (scale bar, 100 nm). Lower inset: A schematic diagram of the device. Reprinted with permission from ref 11. Copyright 2002 Springer Nature. (d) Coulomb blockade and other single-electron phenomena in single-molecule devices with graphene electrodes. Reprinted with permission from ref 53. Copyright 2017 American Chemical Society. (e) Multiple redox-state phenomena in a robust graphene-zinc-porphyrin molecule-graphene transistor. Reprinted with permission under a Creative Commons Attribution 3.0 Unported License from ref 54. Copyright 2015 Royal Society of Chemistry. (f) Measurements of the differential conductance as a function of V_{s-d} and V_g. Reprinted with permission from ref 55. Copyright 2003 Springer Nature.

If the wave functions of molecules have little mixed with the electronic states of electrodes, there is no charge transfer or integer charge transfer between the molecules and electrodes. Charge transfer in this weak coupling regime shows a two-step process in which electrons hop from the metal electrode to the molecular "island," then from the island to the other electrode. For strong coupling, the electronic states of the molecule and electrode overlap significantly, and there is a partial charge transfer between the molecules and electrodes, resulting in a significant broadening of the molecular energy levels. Therefore, electrons could efficiently transport from one electrode to another without stopping on the molecules, which is known as a one-step coherent process.

https://doi.org/10.1021/acsnano.1c11433
ACS Nano XXXX, XXX, XXX−XXX

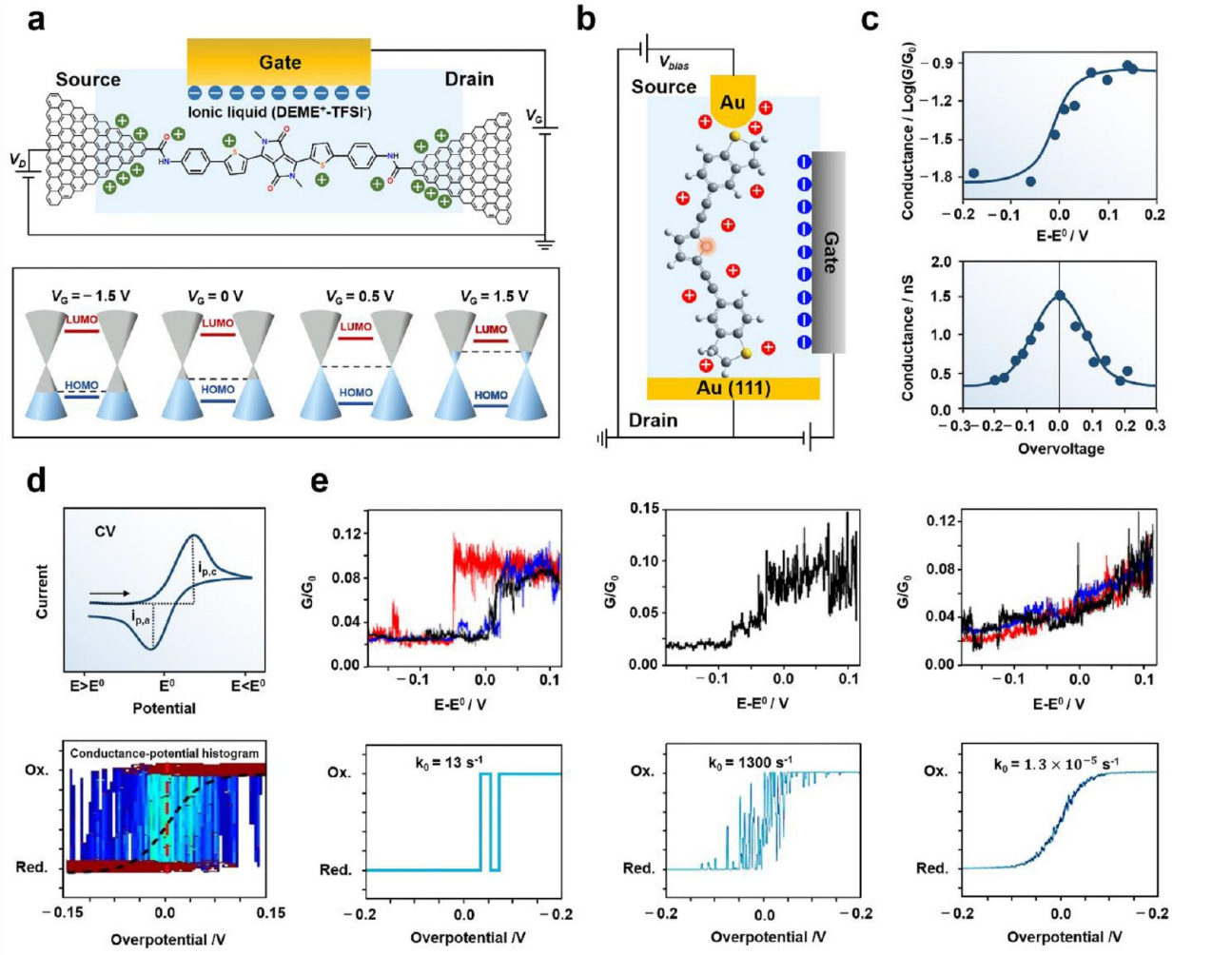

Figure 3. (a) Energetic diagram and device structure of single-molecule devices with an ionic liquid gate. Reprinted with permission from ref 56. Copyright 2018 Wiley-VCH. Reprinted with permission from ref 57. Copyright 2020 Wiley-VCH. (b) Schematic diagram of the electrochemically gating single-molecule conductance of heterocyclic molecules by STM-BJ. Reprinted with permission from ref 61. Copyright 2021 American Chemical Society. (c) One-step resonant tunneling and two-step electron transport mechanisms. Reprinted with permission from ref 63. Copyright 2019 National Academy of Sciences. Reprinted with permission from ref 64. Copyright 2015 American Chemical Society. (d) Stochastic large conductance fluctuations between reduced and oxidized states in a two-step process of electron transfer. Reprinted with permission from ref 60. Copyright 2020 Elsevier. Reprinted with permission from ref 63. Copyright 2019 National Academy of Sciences. (e) Measured and simulated conductance vs potential sweeps for single molecules. Reprinted with permission from ref 63. Copyright 2019 National Academy of Sciences.

Furthermore, the electrical characteristics of molecular junctions, especially molecular conductance, are closely related to the coupling strength of molecule−electrode interfaces, which is demonstrated by the Landauer formula. Specifically, the conductance (G) of molecular junctions can be described as follows:

$$G = \frac{I}{V} = \frac{2e^2}{h} T_L T_R T_{mol}$$

where I is the current through the junction, V is the applied bias and T_L, T_R, and T_{mol} are the transmission coefficients of the left interface, the right interface and the molecule, respectively.

Particularly, in a three-terminal device, the gate voltage can regulate energy-level shifting, which causes resonance between the energy levels of the molecule and electrode, resulting in charge transfer, which is known as resonant tunneling. Furthermore, the strength of the molecule−electrode interface coupling affects electron transport.

When the molecule−electrode interface coupling is strong, charge transport is coherent, and when the coupling is weak, it is incoherent. For weak coupling, if the energy levels between molecule and electrode do not match, electron transport will be blocked. This phenomenon is known as Coulomb blockade (Figure 1b), which forms classic Coulomb diamonds in differential conductance maps. Furthermore, the gate voltage can be varied to bring the narrow molecular energy levels into resonance with the Fermi level of the electrodes, allowing the electron to transport through the molecule. However, for strong coupling, the Coulomb blockade will be broken down, and the gate voltage has little effect on charge transport.[6]

Monitoring of Gate-Controlled Charge Transport Processes. As previously stated, the coupling strength and related energy-level positions between the molecules and electrodes are the critical factors affecting charge transport in

https://doi.org/10.1021/acsnano.1c11433
ACS Nano XXXX, XXX, XXX−XXX

single-molecule devices. Here we summarize the research on monitoring the gate-controlled charge transport processes in different systems, including solid and liquid-gate single-molecule devices.

Solid-Gate Single-Molecule Devices. Solid-gate single-molecule devices are composed of a conductive gate electrode, a high-*k* solid dielectric layer (e.g., aluminum oxide), and source/molecule/drain junction. A three-terminated single molecular transistor has been created by bridging 1, 4-benzenedithiol (BDT) with a delocalized aromatic ring molecule into gold electrodes.[51] Charge transport modulated by an external gate voltage can be directly monitored with the single-molecule device (Figure 2a). Tunneling transport, which is electron transfer from one electrode to another in one step, is the charge transport mechanism for this system. When a molecular orbital enters the conductive window, it develops a resonance-enhanced coupling to the nearest molecular orbital, resulting in increased conductance. However, Coulomb blockade can be observed for the weak coupling system leading to the two-step process of charge transport. For instance,[52] when additional methylene groups are inserted between the molecular π-electron system and metal electrodes, the two-step electron transport process can be monitored using a field-effect transistor device composed of oligophenylenevinylene derivatives (OPV3) and metal (e.g., Au or Pb) source/drain electrodes (Figure 2b). Specifically, the introduction of methylene reduces molecule−electrode interface coupling, causing the system to operate in a weak coupling regime. Therefore, the transport mechanism changes from coherent tunneling to incoherent transport with Coulomb blockade, and the charge transport efficiency is reduced by several orders of magnitude in an off-resonance regime. Similarly, when using the molecule containing a Co ion,[11] the coupling strength between the ion and gold electrodes can be regulated by changing the length of the alkyl chain, which provides a platform for monitoring single-electron phenomena such as Coulomb blockade (Figure 2c).

In addition to single-molecule devices with metal electrodes, graphene electrodes can be used to monitor Coulomb blockade and other single-electron phenomena. Compared with metal electrodes, graphene electrodes are more stable and can be regulated by gating. For example, single-molecule devices can be achieved (Figure 2d) by connecting single extremely short molecules such as 1,4-diaminobenzene or 4,4′-diaminobiphenyl (∼0.6 and ∼1.0 nm, respectively) to graphene nanogap electrodes.[53] Even at room temperature, it is possible to monitor single-electron transport with a large energy Coulomb blockade related to the molecular length and gate voltage. This is also due to the insensitivity of the molecular junction to the atomic configuration of graphene electrodes. Furthermore, because of the stability of graphene electrodes and specially designed molecules, single-electron phenomena beyond Coulomb blockade can be observed including multiple redox states (Figure 2e).[54] Note that for single-electron transport processes with multiple redox states, strong perturbations of intrinsic molecular properties can also be monitored. For instance, electrical transport monitoring is performed on a single-electron transistor device with several redox states, where a single *p*-phenylenevinylene oligomer is placed in a gap of approximately 2 nm wide separating the source and drain electrodes. The presence of the electrostatic image charge effect indicates that even if the electronic overlap between the electrode and molecule is weak, the molecule cannot be conceptually separated from the electrode (Figure 2f).[55]

Liquid-Gate Single-Molecule Devices. In addition to the use of solid-gate devices, liquid-gate single-molecule devices can be used to monitor or understand changes in charge states of single molecules, providing some evidence for elucidating the electron transport mechanism.

Ionic Liquid Gate. Single-molecule devices with an ionic liquid gate usually contain an ionic liquid electric double layer because of the matching sizes of the ions and molecules, so the molecular energy levels can be finely regulated. Similar to solid-state gate devices, charge transport can be detected and controlled in single-molecule devices that use an ionic liquid electric double layer as the gate.

For instance, an ionic liquid gate can effectively regulate the alignment between molecular frontier orbitals and the Fermi energy level of graphene electrodes, thereby tuning the charge transport properties of graphene-based single-molecule junctions. Because gating allows electrons to be repelled and attracted from molecules, it can be used to shift the energy level of molecules into the conductance window, allowing electron transport of molecules in different charged states to be monitored. Therefore, based on GMG-SMJs, the gate-controlled electron transport behavior, including an ambipolar behavior, can be obtained for electrochemically inactive aromatic chain molecules (Figure 3a).[56] Furthermore, the interface coupling strength can be reduced by introducing methylene groups between the molecules and the electrodes. Specifically, by incorporating different numbers of methylene groups between the diketopyrrolopyrrole (DPP) kernel and anchor groups,[57] different charge transport performances can be observed, such as more obvious ambipolar transport. This is because the methylene number parity results in two different connection symmetries between the DPP kernel and graphene electrodes, resulting in different electronic interactions and different relative molecular energy-level alignments from isolated molecules.

Electrochemical Gate. Unlike single-molecule devices with an ionic liquid gate, single-molecule devices using an electrochemical gate generally include an additional reference electrode, and the liquid is a conventional electrolyte solution. In such a device, the regulation of the molecular energy level and electrochemical redox reactions can be realized. Therefore, it is considered a promising platform because the current modulation process can be implemented by directly adjusting the position of the molecular energy level through the ionic double layer, which also leads to the redox reaction caused by electrochemical electron transfer. In the field of electrochemistry reaction kinetics, the Butler−Volmer equation is used to describe the relationship between electrode potentials and current densities that govern the kinetics of redox reactions (Figure 3d).[58−60] However, at the single-molecule level, electron transfer exhibits different characteristics and does not completely follow the Butler−Volmer equation. The one-step resonance tunneling characteristics with enhanced gating performance can be monitored in single-molecule electrochemical devices with fused molecular structures consisting of heterocyclic rings of furan, thiophene, or selenophene (Figure 3b),[61] by adjusting the coupling of different heterocyclic centers to electrodes. The electron transport process mediated by the empty molecular state can be monitored in a single-molecule n-type electrochemical transistor with a single perylene tetracarboxylic diimide

https://doi.org/10.1021/acsnano.1c11433
ACS Nano XXXX, XXX, XXX−XXX

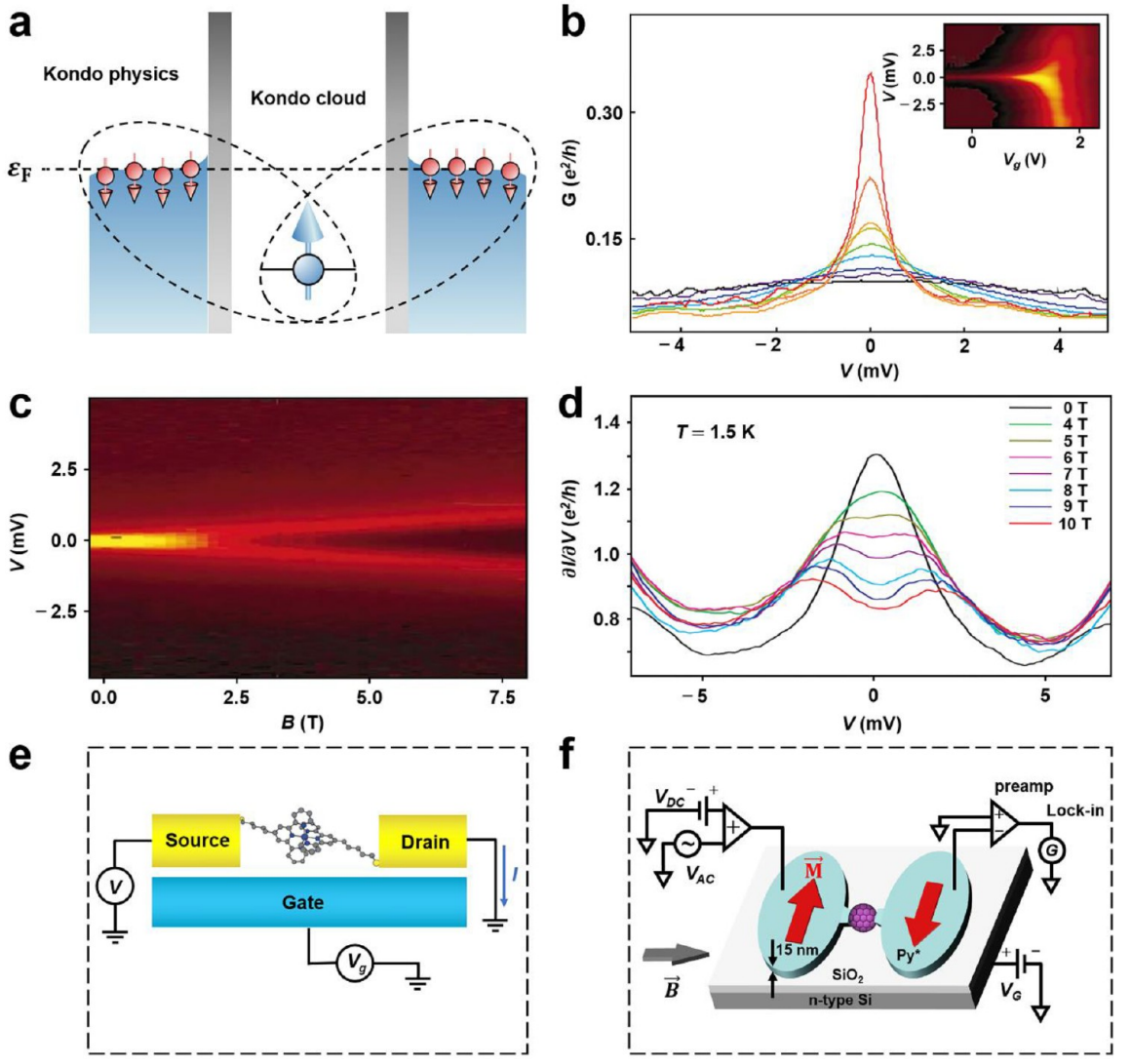

Figure 4. (a) The Kondo effect (left part) originates from the formation of a many-body spin singlet between the spins residing on the molecule and the conduction electrons, leading to screening within the Kondo length. Reprinted with permission from ref 6. Copyright 2019 Springer Nature. (b) Conductance (G) versus V with $V_g = -2.25$ V at various temperatures and (c) Zeeman splitting caused by magnetic fields. Reprinted with permission from ref 70. Copyright 2002 Springer Nature. (d, e) Magnetic-field dependence of the Kondo peak and the device structure. Reprinted with permission from ref 11. Copyright 2002 Springer Nature. (f) Device setup for low-temperature transport measurements. Reprinted with permission from ref 71. Copyright 2017 American Physical Society.

molecule wired to two gold electrodes, in which the current increases significantly.[62] There are two mechanisms for predicting the maximum current near the reduction potential, one is resonant tunneling as described above, and the other is two-step electron transport. First, an electron transfers from one electrode to the redox center through a Franck−Condon transition, then the molecule reorganizes because of environmental and internal relaxation within the adiabatic limit, and finally the electron transfers from the redox center to another electrode (Figure 3c).[63,64] This two-step process of electron transfer is manifested as stochastic large-conductance fluctuations between reduced and oxidized states at the single-molecule level. Moreover, in this case, the electrochemical gating of the single-molecule junction follows the Butler−Volmer equation. The stochastic individual electron-transfer process, which depends on the length of the molecule can be monitored by varying the number of CH_2 groups used to regulate the interface coupling (Figure 3d).[63] Specifically, electron transport is mediated from sequential or coherent electron transfer to incoherent transport via redox states of the molecule as the number of CH_2 increases. The transition from oxidation to reduction occurs instantaneously in devices with long-chain molecules, which operate in a weak coupling regime, whereas it is a sequential process for short-chain molecules that operate in a strong coupling regime. Furthermore, the average conductance against potential in the short-chain system has a sigmoidal dependence, which can be described by equilibrium electron transfer and Nernst equation, but not by incoherent two-step sequential hopping and coherent one-step tunneling (Figure 3e).

MONITORING OF SINGLE-MOLECULE SPIN PROPERTIES

Spin is a natural quantum variable of matter because it is an inherent characteristic of electrons. It is critical to the electronic structure of atoms and molecules, and it endows

https://doi.org/10.1021/acsnano.1c11433
ACS Nano XXXX, XXX, XXX−XXX

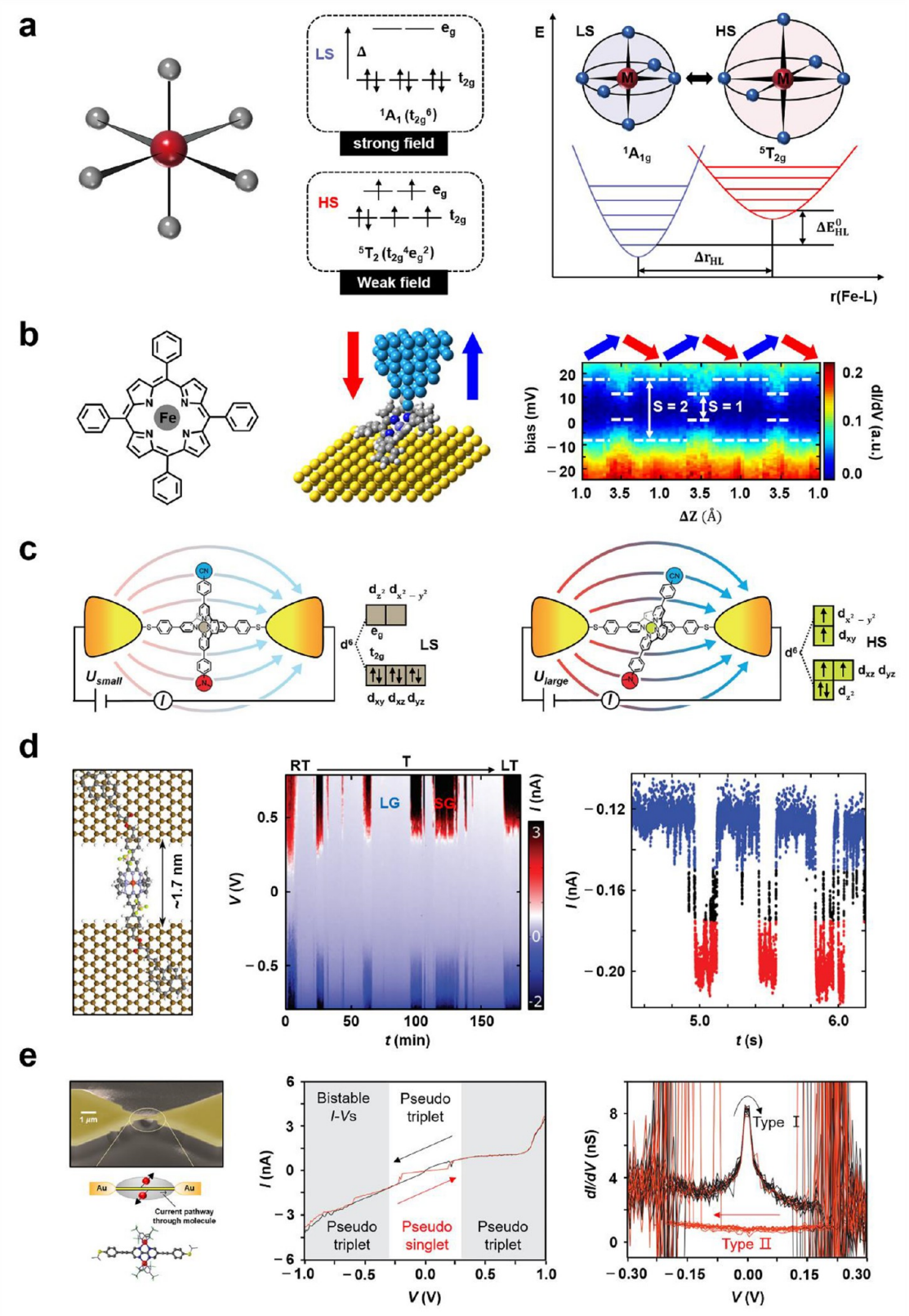

Figure 5. (a) The spin-crossover phenomenon. Reprinted with permission under a Creative Commons Attribution 3.0 Unported License from ref 72. Copyright 2015 Wiley-VCH. (b) Schematic illustration and dI/dV spectra in a FeP molecular junction. Reprinted with permission from ref 17. Copyright 2017 American Chemical Society. (c) Sketch of the voltage-triggered spin crossover switch in a single-molecule junction. Reprinted with permission from ref 76. Copyright 2015 Wiley-VCH. (d) Schematic, temperature, and time bistability of a graphene/Fe-spin crossover/graphene single-molecule junction. Reprinted with permission from ref 78. Copyright 2018 Royal Society of Chemistry. (e) Bistable I–V characteristics due to hysteresis of the coupled spin pair. Reprinted with permission from ref 80. Copyright 2013 Springer Nature.

https://doi.org/10.1021/acsnano.1c11433
ACS Nano XXXX, XXX, XXX−XXX

the material with many useful properties, such as the spontaneous magnetization of magnetic metals. Many monitoring techniques of electron spin and related properties are used in single-molecule electronic devices. This section introduces some of the latest studies on the monitoring of single-molecule spin properties, such as the Kondo effect, Zeeman splitting, and spin crossover.

Kondo Effect and Zeeman Splitting. In the 1930s, it was discovered that the resistance curve of metal-containing magnetic impurities has a minimum value at low temperatures, which is caused by the Kondo effect.[65] However, when the temperature is lower than a certain temperature, the resistance will suddenly increase because of the multiple scattering processes of magnetic atoms and conduction electrons. Similarly, when the electronic state of the molecule has nonzero spin or degeneracy in a single-molecule device, the Kondo effect can cause a significant zero-bias Kondo resonance in conduction.[66] This is due to the exchange interaction between the localized spins in the molecule and conduction electrons in metal electrodes. Specifically, when a spin electron is located on a molecule, an electron cloud is formed on the electrodes, which has a spin polarization that is antiparallel to the spin electron (Figure 4a). This formation of the Kondo screening cloud enhances the density of states in the electrodes, resulting in a high-conductance state below Kondo temperature (T_K). The Kondo temperature is defined as

$$T_K = 0.5(\Gamma E_C)^{1/2} \exp(-\pi\varepsilon/\Gamma)$$

where E_C is the charging energy, Γ is coupling parameter of molecules and electrodes, and ε is the difference between the localized state and the Fermi level of the electrodes.

Because the external magnetic field can lift the degeneracy of the up and down spin states, the energy levels of the spin electron are split, which is known as Zeeman splitting. By applying a finite bias to a single-molecule device under the application of a magnetic field, the splitting of the original Kondo resonance peak can be revealed.[6,8,67−69]

Therefore, single-molecule devices can be used to monitor electron spin characteristics, such as the Kondo effect and Zeeman splitting as described above. Early reports of these effects can be traced back to transistors based on electromigration single-molecule junctions. The Kondo effect can be observed in single-molecule transistors that use molecules containing a Co ion with spin electrons bonded to polypyridyl ligands and attached to insulating tethers of different lengths as conductive channels (Figure 4d,e).[11] Furthermore, the reversible regulation process of the Kondo resonance can be achieved through gate voltage bias, which can alter the charge and spin states of molecules in single vanadium transistors (Figure 4b).[70] Furthermore, Zeeman splitting can be observed in this single-molecule device (Figure 4c), where the magnitude of Zeeman splitting as a function of magnetic field (B) is $g\mu_B B/e$, where g represents gravity constant, μ_B represents magnetic permeability, B is magnetic flux density, and e is element charge. Similarly, by measuring the low-temperature transport of C_{60}-based single-molecule transistors with ferromagnetic electrodes, the effect of manipulating the magnetization of the electrodes on the Kondo effect can be accurately monitored (Figure 4f).[71] Specifically, the orientation of the magnetization distribution can be controllably switched between parallel and antiparallel through specially designed ferromagnetic electrodes. The exchange between the local spin in the molecule and the spin electron in the ferromagnetic electrode can be affected because of the transition from parallel to antiparallel, resulting in different gate-controlled Kondo resonance characteristics.

Spin Crossover. Spin crossover, also known as spin transition, can switch molecules between low-spin (LS) and high-spin (HS) states. The two states of spin-crossover molecules can be distinguished by different magnetic, optical, and structural properties, and they can be transformed into each other by external disturbances such as temperature, light, pressure, magnetic field, or inclusions of guest molecules. This section mainly introduces the basis of spin crossover as well as the monitoring and regulation of molecular spin-state transitions by single-molecule junctions.

Basics of Spin Crossover. Molecular materials with adjustable spin states have piqued the interest of researchers because of their significant applications, such as switches, sensors, high-density information storage, and display. The phenomenon of spin crossover is one of the most significant manifestations of spin control. Generally, spin crossover molecular systems involve octahedral complexes formed by first-row transition-metal ions with a $3d^n$ (n = 4−7) electronic configuration, which can achieve the reversible conversion between LS and HS states under certain external stimuli. Such spin conversion depends on the ligand field energy and the spin pairing energy of the complexes (Figure 5a).[72] According to crystal field theory, the interaction between the central atom of the complexes and the ligand is similar to the electrostatic interaction between the positive and negative ions in an ionic crystal. The electrostatic potential field formed by the ligand in the octahedral complex affects the distribution of d-electrons in the central ion, causing the five spin-degenerate levels to split into e_g and t_{2g} orbitals in the ligand field. The energy difference between two sets of d-orbitals is defined by the crystal field splitting energy (Δ). Furthermore, another type of energy was produced by putting two electrons into the same orbital, known as spin pairing energy (P). For strong field ligands ($P < \Delta$), electrons can occupy the low-energy t_{2g} orbital, resulting in fewer unpaired electrons. However, for weak field ligands ($P > \Delta$), electrons will occupy different orbitals, resulting in the appearance of many unpaired electrons. The former is defined as the LS state and the latter as the HS state. Currently, iron(II), d^6, is the most commonly used transition-metal ion for studying the thermal spin-crossover phenomenon. The metal-to-ligand bond distances and the molecular volume are increased as the temperature rises. Therefore, the interaction between the metal and ligand weakens, causing the electron configuration to change from $(t_{2g})^6(e_g)^0$ to $(t_{2g})^4(e_g)^2$, that is, the spin state transfers from LS to HS. The potential energy diagram along the metal−ligand stretching coordinate shows that the potential wells of the HS and LS states are separated horizontally and vertically. When the energy difference for the two spin states meet certain conditions, such as $\Delta E^0_{HL} \approx K_B T$, the thermal spin crossover can be observed (Figure 5a).[73] Therefore, spin-crossover molecules are ideal candidates for implementing spintronic devices at the molecular level. Single-molecule devices provide an ideal platform for studying spin-state changes of spin-crossover metal complexes, which can accurately monitor and control a single spin state.

Monitoring of Spin Crossover in Single-Molecule Devices. In single-molecule junctions, spin-crossover transitions are usually accompanied by simultaneous changes in molecular geometry and electronic configuration, which

https://doi.org/10.1021/acsnano.1c11433
ACS Nano XXXX, XXX, XXX−XXX

significantly affect molecular conductance. Therefore, monitoring the spin-crossover phenomenon through single-molecule devices is highly recommended. The spin-crossover *trans*-bis(isothiocyanato)iron(II) complex sandwiched between gold electrodes is used to calculate coherent transport properties using density functional theory combined with a non-equilibrium Green function procedure, which shows that the conductivity of HS states is greater than that of the LS state.[18] Furthermore, when $[FeL_2]^{+2}$ complex is incorporated in the electrodes, where L is a 2,2′:6,2″-terpyridine group, the reduction of the HOMO−LUMO gap during the phase transition increases the current response to spin change by 4-orders of magnitude, which is equivalent to a magneto-resistance effect of over 3000%.[74] These characteristics enable the investigation of spin crossover in single-molecule devices.

Monitoring and regulating spin states of spin-crossover molecules in single-molecule devices has achieved significant progress using external stimuli, such as mechanical manipulation, temperature, and electric field. Mechanically controlled spin crossover is often accompanied by a change in coordination bond length between central metal ion and ligand, resulting in a change in the ligand field energy. For instance, in stretching-induced single-molecule switches based on the Fe^{II} terpyridine complexes, the large enough change in the spatial arrangement between the two terpyridine ligands that depend on the electrode spacing may distort the Fe^{II} coordination sphere and thus trigger the transition from the LS (S = 0) state to the HS (S = 2) state. Meanwhile, the LS-HS transition can be reflected in the single-molecule junction conductance. Numerous molecular junctions formed with Fe^{II} terpyridine complexes can increase conductance.[75] Furthermore, the mechanically controlled interconversion between different molecular conformations can be used to induce spin crossover in single-molecule devices. For instance, when widening molecular junction gap width by increasing the STM tip height, the conformation shift from the saddle to the planar of a single Fe-porphyrin molecule shortens the metal−ligand bonds, resulting in Fe spin-state transition from HS to LS. Meanwhile, the line shape of zero-bias resonance associated with the Fe spin state changes reversibly from wide (HS) to narrow (LS) with a junction gap (Figure 5b).[17]

In addition to mechanical manipulation, electric fields have been used to drive spin crossover in single-molecule devices. The switching mechanism of a gating electrode can be divided into two types. One is to apply an electric field force on the molecule inside, distorting the metal ion coordination sphere. For example, one of the two terpyridine ligands arranged vertically fixes a Fe^{II} complex at the end of the electrodes, whereas the other one exhibits an inherent dipole moment, which senses the electric field. When the applied voltage is increased, the metal−ligand distance of $[Fe^{II}(tpy)_2]$ complex increases, which eventually reduces the crystal field interaction. The $I-V$ curve shows a significant hysteresis window around the spin state switching point, demonstrating the spin crossover from the LS state to the HS state in the molecular junction (Figure 5c).[76] The other mechanism is that the occupied ligand levels can be adjusted by increasing the gate voltage, which increases ligand field energy. Spin-crossover phenomenon can be achieved in a three-terminal molecular junction composed of Mn^{2+} ion complexes coordinated by two terpyridine ligands, which have an HS ground state, by adding an electron to the terpyridine ligand system under the action of the gate electrode. This is because the reduction in terpyridine ligands strengthens the coupling strength between the ligands and Mn^{2+} ion complex, which then stabilizes the LS configuration.[77]

Furthermore, temperature induction is another common method for triggering the spin crossover. For Fe (II) complex, which is coordinated with two 2,6-bis(pyrazolyl)pyridine ligands, the spin crossover can be induced by a small temperature disturbance at the molecular level. A change in the ligand−metal ion distance induced by a small temperature perturbation can influence the crystal field splitting energy and thereby initiate conductance bistability between the LS and HS states (Figure 5d).[78]

The above-mentioned molecular systems are based on a single magnetic center. The polar magnetic molecules formed by two transition-metal ions linked through a chemical group can switch between different spin states, such as a MeO-Cobaltocene dimer. However, this is different from the traditional spin-crossover phenomenon, because two magnetic centers always maintain HS state ($S = 1/2$) and only exchange electrons through the middle linking group with a doubly occupied singlet ($S = 0$) under the electric field. Furthermore, this exchange of singlet and triplet causes electrostatic spin crossover in the two-terminal device under a certain bias voltage, which is also known as singlet-to-triplet crossover.[79] Additionally, in a magnetic molecular switch based on the Co^{2+} ion pair perpendicular to the current pathway through the molecule, the voltage-induced changes in the magnetic exchange coupling pathway between the cobalt sites are the main reason for driving the transition between the pseudosingle state and pseudotriplet state. These states can be distinguished by the absence or presence of a Kondo anomaly at zero bias in the low-temperature conductivity data (Figure 5e).[80]

Generally, the induction of spin crossover can change the ligand field energy applied to complex central ions. Not only can the spin states of transition-metal complexes be observed using the single-molecule device platform but also the spin-crossover phenomenon induced by different external stimuli can be monitored using the conductance characteristics of the devices. This has an important reference significance for developing various types of molecular spin devices.

MONITORING OF CONFORMATIONAL ISOMERIZATION PROCESSES OF SINGLE MOLECULES

Generally, changes in molecular conformation affect their electronic structures and properties. Monitoring changes in molecular conformation is critical for the rational application of molecules in the fields of chemistry, biology, and materials. In traditional characterization methods, ensemble information obscures the behavior of individual molecules. Therefore, it is critical to monitor changes in molecular configuration at the single-molecule level. Single-molecule devices can be used to monitor the structural transformation of single molecules, providing a platform for exploring the process of molecular conformation changes at the single-molecule level. Here, research on the monitoring of stereoelectronic effects, photoisomerization processes, and force-controlled isomerization processes of single molecules is summarized.

Monitoring of Stereoelectronic Effects. A stereoelectronic effect is a critical effect caused by changes in molecular configuration. This effect is the basis of reaction chemistry, it reflects the influence of the relative spatial orientation of electronic orbitals on molecular properties and

https://doi.org/10.1021/acsnano.1c11433
ACS Nano XXXX, XXX, XXX−XXX

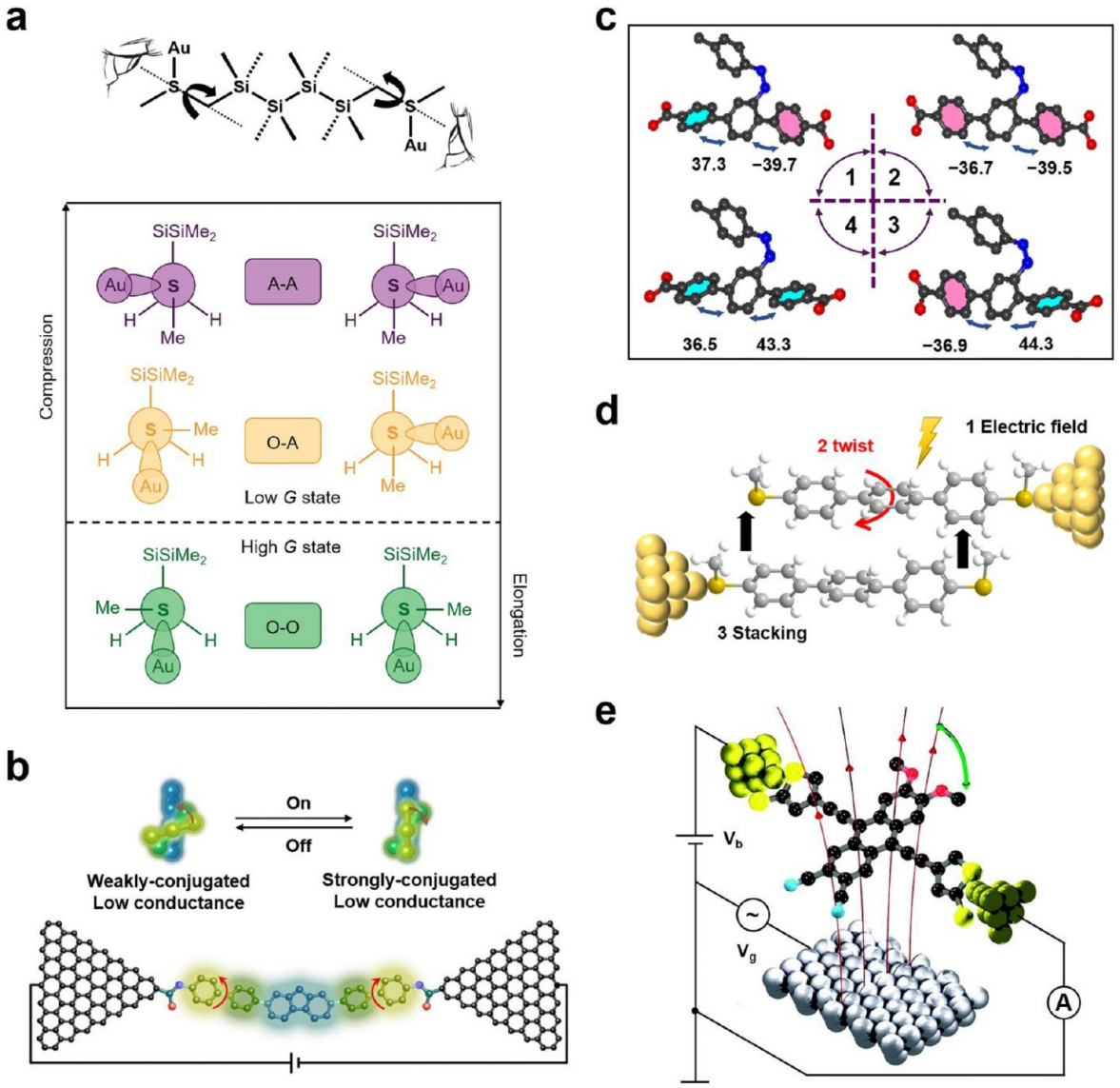

Figure 6. (a) Newman projections for the A−A (purple), O−A (yellow), and O−O (green) dihedral configurations from the perspective of the sulfur−methylene σ bond in the Au−Si_4−Au system. Reprinted with permission from ref 81. Copyright 2015 Springer Nature. (b) Schematic of conformational transition of terphenyl units between strongly conjugated and weakly conjugated states and corresponding hexaphenyl aromatic chain single-molecule junctions. Reprinted with permission from ref 19. Copyright 2017 American Chemical Society. (c) Four stable fine conformations can be observed in an asymmetry device using azobenzene unit as a branch. Reprinted with permission from ref 20. Copyright 2021 Wiley-VCH. (d) Schematic of single-molecule junctions and single-stacking junctions of terphenyl. Reprinted with permission from ref 82. Copyright 2020 American Chemical Society. (e) Design of a molecular motor with a permanent electric dipole moment. Reprinted with permission from ref 83. Copyright 2010 American Chemical Society.

reactivity. Recently, precise control and monitoring of stereoelectronic effects have been achieved at the single-molecule level based on single-molecule junctions. Because of the strong σ conjugation in the oligosilane backbone and the spatial characteristics of the sulfur−methylene σ bonds, there are three dihedral configurations in the Au−molecule−Au system (O−O, A−A, and O−A states) for permethyloligosilanes with methylthiomethyl electrode linkers. Because the A−A and O−A states conformation have similar tunneling coupling, they exhibit a low-conductivity state (Figure 6a).[81] Therefore, the configurations of the three dihedral correspond to the two states of high and low conductances. By analyzing the conductance of the single-molecule junction, the changes in the molecular conformational structure can be monitored. Additionally, the conductance of the junction can be controlled by simply lengthening or compressing the molecular junction, so that the adjustment of the molecular conformation can be monitored.

In addition to the terminal dihedral of the $SiMe_2$ system, the variation of twisting angles between phenyl rings can significantly affect the structure and physical properties of molecules and have a stereoelectronic effect. For example, the stereoelectronic effect of a hexaphenyl aromatic chain molecule has been monitored by single-molecule junctions based on graphene nanogap electrodes (Figure 6b).[19] The twisting of benzene rings at both ends can produce different degrees of conjugation, which leads to changes in conductance. Additionally, the twisting of the benzene ring can be controlled by

https://doi.org/10.1021/acsnano.1c11433
ACS Nano XXXX, XXX, XXX−XXX

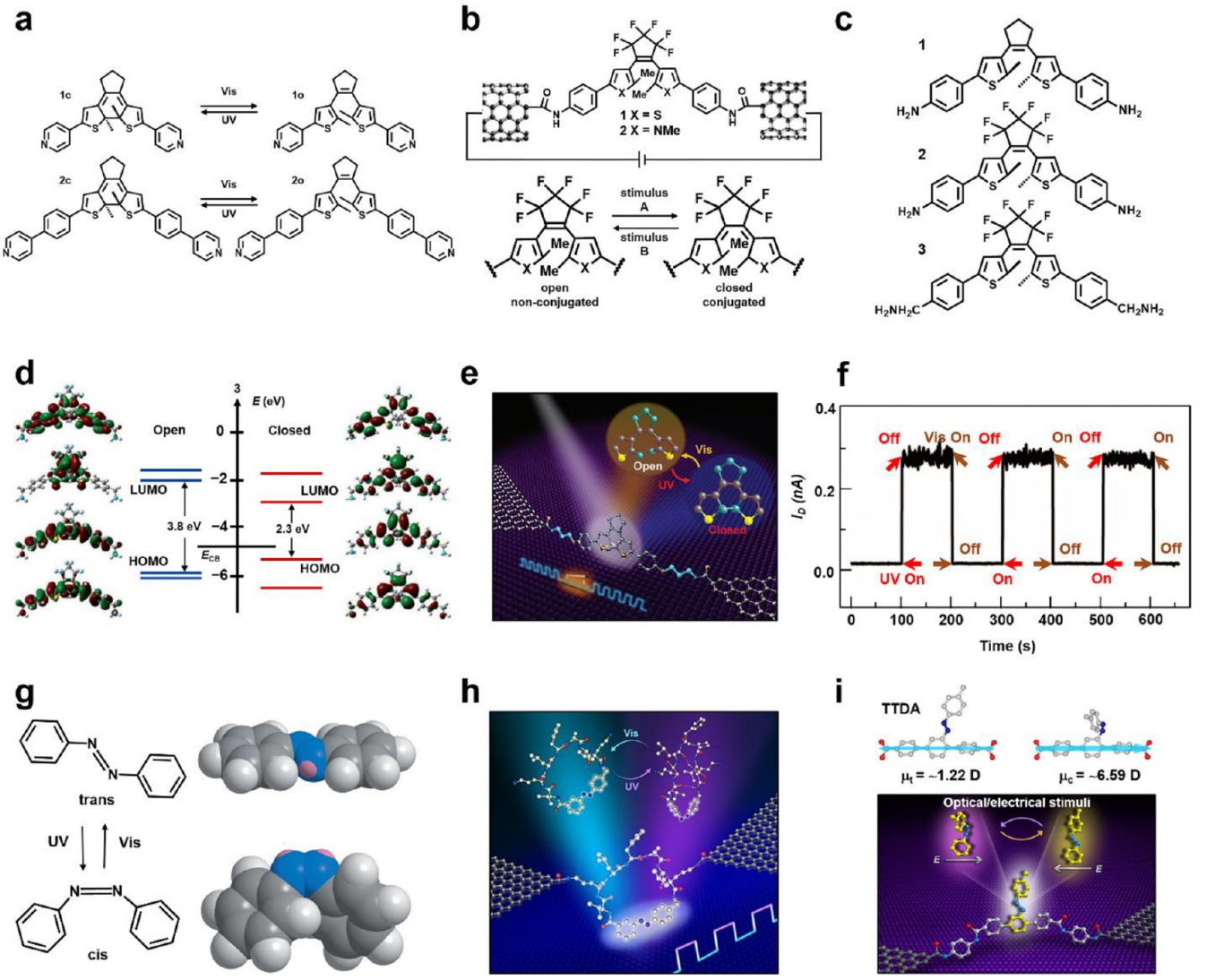

Figure 7. (a) Isomers of the pyridine-terminated diarylethene derivatives. Reprinted with permission from ref 88. Copyright 2011 American Chemical Society. (b) Switching between conjugated and nonconjugated molecular structures. Reprinted with permission from ref 90. Copyright 2007 American Chemical Society. (c, d) Molecular structures, calculated molecular energy levels, and related molecular orbital diagrams of diarylethene with different numbers of methylene groups. Reprinted with permission from ref 91. Copyright 2013 Wiley-VCH. (e, f) Reversible photoisomerization processes of diarylethene molecules. Reprinted with permission from ref 92. Copyright 2016 American Association for the Advancement of Science. (g) Structures and space-filling models of *trans* and *cis* isomers of azobenzene. Reprinted with permission from ref 96. Copyright 2013 Wiley-VCH. (h) Schematic representation of a graphene-single azobenzene-containing peptide molecule device. Reprinted with permission from ref 97. Copyright 2020 Wiley-VCH. (i) Device structure and dipole analysis of a single-molecule device using azobenzene as a side group. Reprinted with permission under a Creative Commons CC-BY license from ref 98. Copyright 2019 Springer Nature.

temperature. Based on the investigation of the electrical characteristics of the single-molecule junction with a hexaphenyl aromatic chain, the twisting dynamics of the benzene ring can be monitored.

As previously stated, the stereoelectronic effect caused by twisting the benzene ring can be monitored by single-molecule junctions. The change process in the subtle molecular structure caused by the introduction of side groups in the molecule can also be monitored because charge transport of the single-molecule junction is very sensitive to the asymmetric electronic structure of the molecule. The introduction of an azobenzene unit as a branch in the central ring of the terphenyl molecule can result in the asymmetry of the molecular structure. By monitoring the current characteristics of the single-molecule junction in real-time, the photoisomerization process of an azobenzene side group can be monitored. Furthermore, four stable conformations can be detected when the azobenzene is in the *cis*/*trans* states (Figure 6c) because of the different angles between the benzene ring on both sides and the central benzene ring.[20] Based on the current−time (I−t) characteristics, the temperature-dependent rotational kinetics of benzene rings can be deduced.

The rotation of the benzene ring can be further regulated and monitored for a bimolecular system with electric field-induced stacking. For example, in single-stacking terphenyl junctions, biomolecular interaction can be adjusted by changing the electric field, and the torsion of benzene rings can be regulated. The dihedral angle of terphenyl decreases as

https://doi.org/10.1021/acsnano.1c11433
ACS Nano XXXX, XXX, XXX−XXX

the electric field strength increases (Figure 6d).[82] In addition to the rotation between benzene rings, the rotation of benzene rings connected by triple bonds in molecules can be effectively monitored and controlled through single-molecule junctions. Molecules with a dipole rotor are connected to nanogap metal electrodes through bidentate mercaptothiophene linking groups, which can be driven to rotate by modulating the electric field generated by the oscillating gate (Figure 6e).[83] The rotation of a molecular machine is monitored by a single-molecule device. Specifically, by adjusting the gate voltage, the molecule can repeatedly switch between two stable states, resulting in changes in conductance. The process of single molecular rotation can be monitored in real-time by investigating the conductance characteristics.

Monitoring of Photoisomerization. Photoisomerization is a key photochemical or photophysical process. Monitoring this process is critical for studying the intrinsic physical and chemical properties of molecules and realizing molecular functionalization. Photochromic molecules with photoisomerization properties can undergo a reversible conformational transition under light with a specific wavelength, so they have attracted widespread interest in optoelectronic devices.[84,85]

Diarylethene has broad application prospects in optoelectronic functional materials as a typical photochromic molecule.[86,87] It is mainly composed of two aromatic heterocycles connected by carbon−carbon double bonds and has two reversible structures of a nonconjugated open state and a conjugated closed state. Under ultraviolet light, diarylethene changes from a nonconjugated open state to a conjugated closed state, and the molecular conductance correspondingly changes from low to high states. When diarylethene is irradiated with visible light, it can be restored to nonconjugated open states. By using diarylethene molecules with pyridine electrode linkers, based on STM-BJ technology to study the electronic characteristics, the high conductivity state corresponding to the conjugated closed state of the molecule is monitored (Figure 7a).[88] However, for the nonconjugated open state, it is impossible to measure the specific conductivity value because the conductivity of the molecule is lower than the detection limit of the instrument. Additionally, as reported in previous studies, photoisomerization in single-molecule devices based on metal electrodes can only achieve unidirectional changes. Specifically, diarylethene can change from closed to open states under visible light irradiation, but cannot return to the closed state under ultraviolet light. This is because the orbital between the molecule and electrode is highly hybridized and the electrode quenches the photoexcited state of the open-state diarylethene molecule.[89]

In addition to metal electrodes, single-molecule devices based on carbon electrodes can be used to monitor the photoisomerization properties of diarylethene molecules. For example, to construct devices using diarylethene molecules based on thiophene and pyrrole, the conjugated molecules are covalently integrated into single-walled carbon nanotubes (SWNTs) through amide bonds (Figure 7b).[90] The conductivity of a single-molecule junction ranges from low to high states under ultraviolet irradiation, which proves that the transition process of thiophene configuration from open to closed states is successfully monitored. However, thiophene cannot switch from closed to open states under visible light irradiation. This is in contrast to the case based on metal electrodes, highlighting the importance of the molecule−electrode interface.

To achieve the reversible photoisomerization process of diarylethene molecules, a series of attempts have been made, including the use of graphene electrodes, adjustment of the energy-level alignments, and interface coupling of the molecule−electrode interface. For example, fluorinated cyclopentene is used to replace the hydrogenated unit in graphene-based single-molecule junctions. Although the energy level is lower because of the electron-withdrawing effect of the fluorinated unit, the reversible configurational changes of diarylethene molecule between the open and closed states still could not be realized.[91] A methylene group (CH_2) is introduced between the terminal amine group and the functional center on each side (Figure 7c) to weaken the interface conjugation.[91] The configuration of two molecules from open to closed states can monitor current−voltage ($I-V$) characteristics based on single-molecule junctions. Although CH_2 groups reduce π-electron delocalization, it is still unable to achieve the reversible configuration change between the open and close states of diarylethene in single-molecule junctions (Figure 7d). Three methylene groups are introduced between the diarylethene functional center and terminal amine groups to optimize the interface coupling to reduce quenching.[92] Through the electrical characterization, two states of high and low conductance are observed, corresponding to the closed and open isomers (Figures 7e,f). The reversible photoisomerization processes of diarylethene molecules are successfully monitored in single-molecule junctions. Additionally, the temperature-dependent charge transport mechanism of carbon electrode-diarylethene single-molecule junctions has been explored. The single-molecule junctions in both forms exhibit a transition from low-temperature coherent tunneling to high-temperature incoherent transport because of the thermally activated rotation of benzene rings at both sides of molecules.[93]

Azobenzene is a typical photochromic molecule in addition to diarylethene molecules, which performs the photoinduced *cis*−*trans* isomerism effect under ultraviolet or visible light.[94,95] Specifically, when it is exposed to ultraviolet light, it transforms from a planar *trans* configuration to a bent *cis* configuration (Figure 7g).[96] Single-molecule junction provides an effective method for monitoring the configuration changes of azobenzene. There are two cases where the azobenzene unit is located in the main or side chain of the molecule. When azobenzene is on the main chain, the configuration change of azobenzene can change the molecular properties. Additionally, configuration monitoring can be performed for molecules containing azobenzene units. Configuration changes of azobenzene can cause changes in conductance because of the difference in structures. Specifically, the *trans* configuration corresponds to high conductivity, and the *cis* configuration corresponds to low conductivity. Through the investigation of the conductivity characteristics based on the graphene-based single-molecule device, the change in conductance proves that the azobenzene unit can be reversibly switched between *trans* and *cis* configurations.[96] Constructing label-free single-molecule devices containing single peptides and real-time conductance measurements can infer their structural dynamic behavior, which is important in understanding the inherent dynamic behavior of proteins. The configuration of azobenzene switches between *cis* and disordered *trans* isomers under ultraviolet light and visible light by covalently attaching an

https://doi.org/10.1021/acsnano.1c11433
ACS Nano XXXX, XXX, XXX−XXX

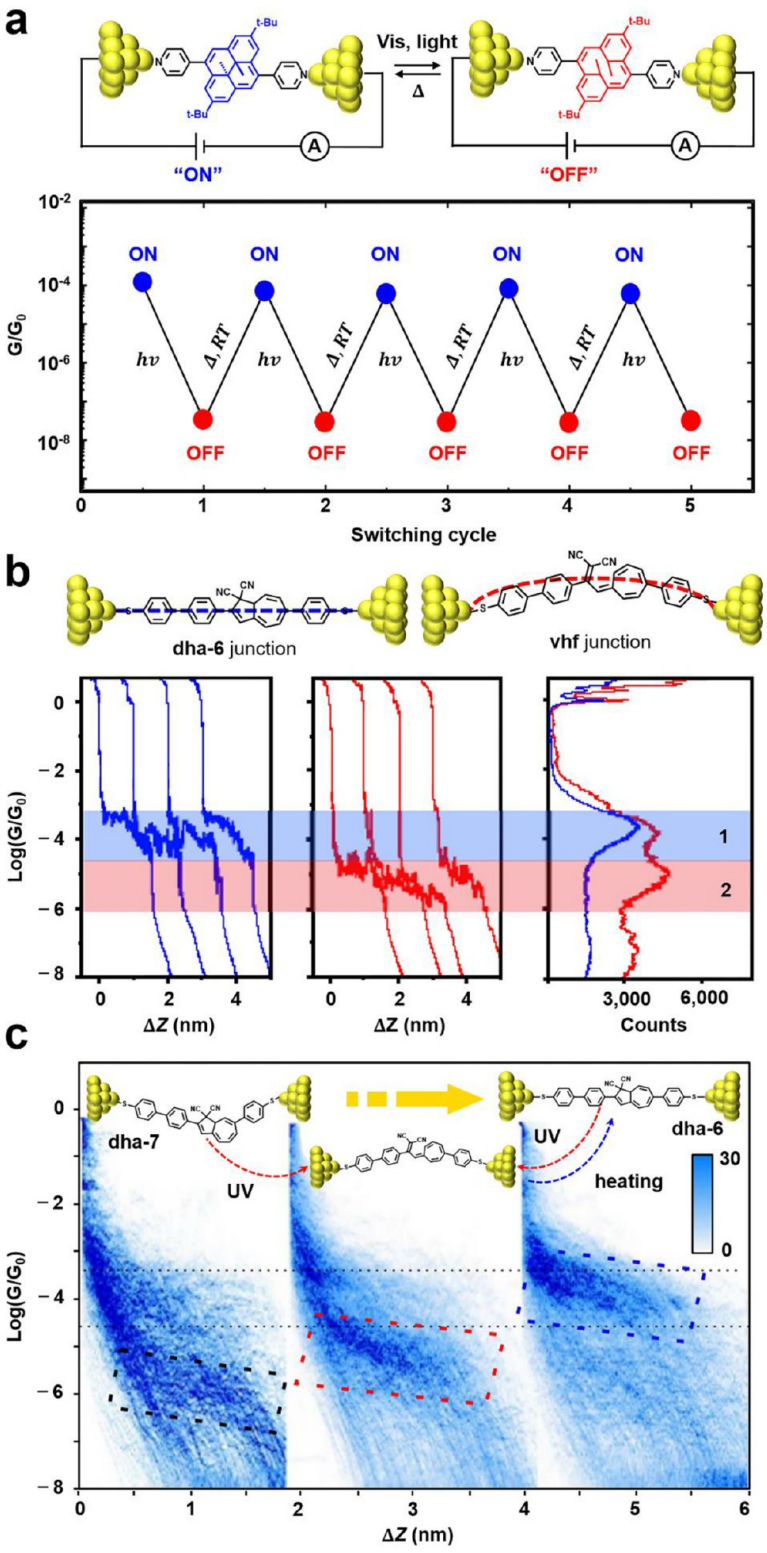

Figure 8. (a) Isomers of the pyridine-dimethyldihydropyrene. Reprinted with permission from ref 99. Copyright 2013 American Chemical Society. (b, c) Schematic, typical individual conductance-distance traces and 2D conductance-displacement histograms in dihydroazulene break junction. Reprinted with permission under a Creative Commons CC-BY license from ref 100. Copyright 2017 Springer Nature.

azobenzene-containing peptide molecule into graphene nanogap electrodes. Real-time conductivity measurements show that each isomer has three different states, which proves that the molecular configuration changes are monitored (Figure 7h).[97]

In addition to using azobenzene as the core of molecules, molecules with azobenzene units as a side group can monitor the process of configuration changes through single-molecule junctions. Azobenzene is introduced into the terphenyl species as a side group, and the molecule with amino end groups is

https://doi.org/10.1021/acsnano.1c11433
ACS Nano XXXX, XXX, XXX−XXX

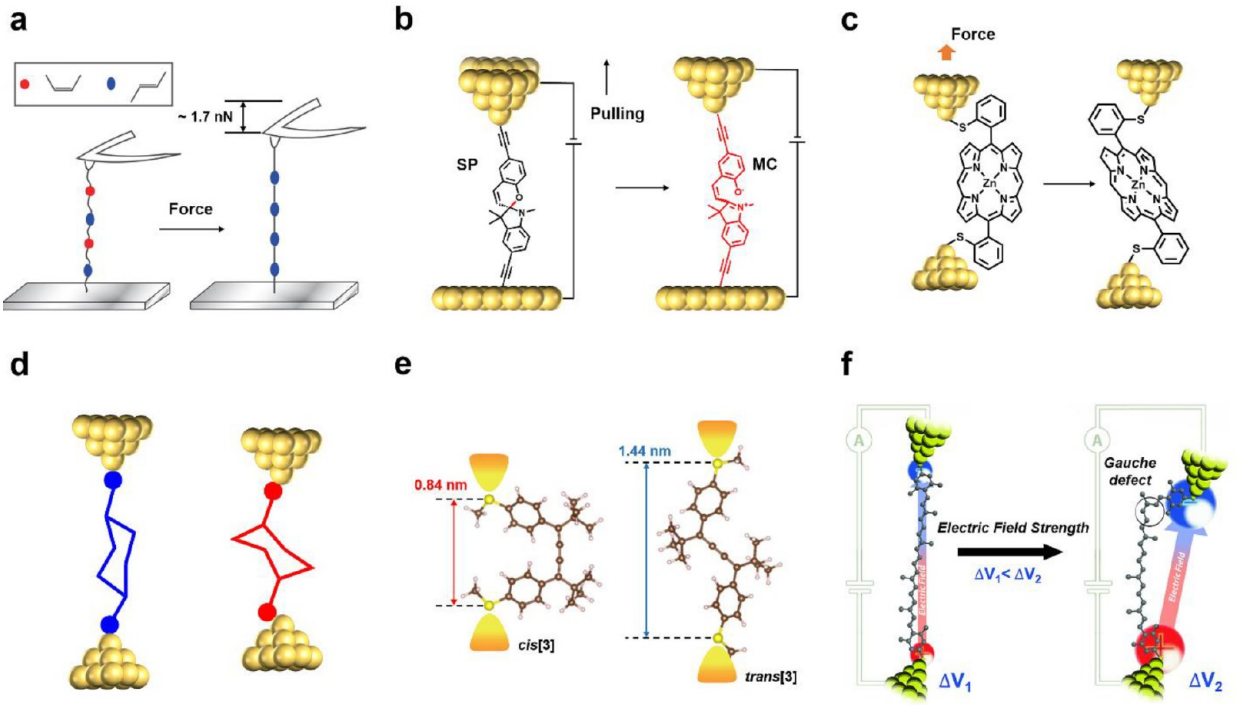

Figure 9. (a) Schematic diagram of the AFM-based single molecule force spectroscopic experiment. The *cis* alkene (red) is directly converted to the *trans* isomer (blue) at a force of ∼1.7 nN in a polymer. Reprinted with permission from ref 108. Copyright 2017 American Chemical Society. (b) Schematic diagram describing the operation of the isomerization process by mechanical force. The C−O bond (red) is broken. Reprinted with permission from ref 112. Copyright 2019 American Chemical Society. (c) Schematic diagram of the force-induced conformational transition of the porphyrin molecule with thioacetyl terminal groups at the ortho position. Reprinted with permission from ref 116. Copyright 2018 American Chemical Society. (d) Schematic diagram of the conformational transition of cyclohexane. Reprinted with permission from ref 118. Copyright 2020 Elsevier Inc. (e) Schematic diagram of the *cis*−*trans* isomerization of cumene showing distinct S−S distances. Reprinted with permission under a Creative Commons CC-BY license from ref 119. Copyright 2019 Springer Nature. (f) Schematic diagram of an electric field force-induced isomerization process of tetramethyl carotene. Reprinted with permission under a Creative Commons CC-BY license from ref 120. Copyright 2021 MDPI.

connected between graphene nanogap electrodes through amide bonds (Figure 7i). Because the dipole moment of azobenzene molecules along the main chain direction is different in *trans* and *cis* conformations, the ability of the electric field to regulate the molecular energy is different (Figure 7i).[98] Therefore, the changes in the molecular structure that accompany the changes in the dipole properties are manifested by the changes in conductance. Furthermore, the process of subtle molecular structural change can be monitored. The photoisomerization process of azobenzene side groups can be monitored under ultraviolet or visible lights using real-time current characteristics.[20]

In addition to diarylethene and azobenzene molecules, the configuration changes of other photoisomerized molecules can be monitored on the basis of single-molecule devices. Dimethyldihydropyrene (DHP) is a polycyclic π-conjugated unit, which can reversibly switch between a colorless open state and a more stable closed state under different specific wavelengths of light. Pyridine groups are introduced on both sides of DHP for constructing single-molecule junctions. Because of the different degrees of conjugation, the two isomers of pyridine-DHP correspond to high and low conductivity (Figure 8a). Based on the study of electronic properties of mechanically controlled break junctions, the molecular conductivity can be reversibly converted between high and low conductivity because of the two isomers under different wavelengths of light treatment (Figure 8a).[99] Additionally, dihydroazulene exhibits light control properties. Similarly, the configuration changes in dihydroazulene can be monitored based on the conductance states detected by STM-BJs because of the two states with high and low conductance (Figure 8b).[100] Through statistical analysis of the conductivity characteristics, the reaction kinetics can be monitored (Figure 8c). Furthermore, spiropyran (SP) derivatives can be isomerized under specific wavelengths of light.[101] Two states of high and low conductance are observed through electrical characteristics, corresponding to the two configurations. Therefore, the photoisomerization process of SP derivatives can be monitored.

Monitoring of Force-Controlled Isomerization. Recently, the regulation of molecular conformation by mechanical force has gradually become a burgeoning interdisciplinary subject, including mechanical discoloration,[102,103] mechanical catalysis,[104] small molecule release,[105] force-induced stress enhancement,[106] and mechanical luminescence.[107] Single-molecule devices represented by metal junctions provide a favorable platform for in-depth research in this field because of their characteristic structural advantages. For instance, AFM technology is a common monitoring method to study the effect of the process of molecular isomerization by force. In the process of stretching the polymer containing C═C bond with an AFM probe, *cis* olefins can be directly converted to *trans* olefins on the time scale of ∼1 ms under the tension of ∼1.7 nN at room temperature (Figure 9a).[108] The reason is that the

https://doi.org/10.1021/acsnano.1c11433
ACS Nano XXXX, XXX, XXX−XXX

olefins are induced to produce a double radical intermediate state by force, which affects the process of *cis*−*trans* transformation.

Spiropyrans have been widely used in the construction of functional monomolecular devices over the past decades because of their intrinsic molecular advantages.[109−111] Ring-closed SP can be transformed into zwitterionic merocyanine (MC) in the ring-open state, and conjugation is absent between the two heterocycles in the ring-closed molecular structure. SP can be transformed into MC through accurate regulation of the external force. The conjugation effect can be generated between the chromene and indoline portion parts in the molecular structure. Therefore, compared with the ring-closed state, the ring-open state has higher conductivity. The conversion between closed and open states is caused by the cleavage of helical C−O bond, which can lead to the isomerization of the distorted *cis*-MC into the most planar *trans*-MC. The study of single-molecule electrical switches based on SP mechanical stimulation has been electrically monitored using the STM-BJ platform. A SP derivative with alkynyl ends has been investigated. In the neutral solvent without light, with the increase of the electrode spacing, the molecular current first decreases and then increases suddenly, indicating that the C−O bond is broken under the action of the external force to form zwitterionic MC. Because of the stronger Au−C bond formed between SP and the electrode, switching between the closed SP state and the open MC states can be achieved through tensile strain (Figure 9b).[112] Similarly, the isomerization process of SP caused by mechanical stimulation can also be monitored using the MCBJ method. The conversion of *I*−*V* characteristics from rectification to symmetry can be realized, and the corresponding SP is isomerized to MC by mechanical stimulation induced in the process of breaking the junction.[22]

Porphyrins are a class of organic heterocyclic compounds, which have attracted much attention in the fields of nanoscience and molecular electronics.[113−115] Through *ortho*-substituents (Figure 9c), 5,15-diaryl porphyrin, which combines thioacetyl (SAC) or methyl sulfide (SME) groups on the *ortho*-position of the outer benzene ring, produces two *cis* and *trans* atropisomers of each compound.[116] These atropisomers cannot be converted to each other in solution at room temperature. However, using STM-BJ technology, the isomerization of *cis* thioacetyl isomer (SAC) into *trans* isomer can be monitored during the stretching process of the molecular link. The calculation shows that the nonplanar conformation of the junction enhances isomer transformation, and the molecular deformation of the junction between molecules and electrodes has a significant effect on the process of molecular isomerization.

In addition to the rotation of chemical bonds, other molecular isomerism introduced by mechanical forces can be monitored through single-molecule junctions. For example, the two chair isomers of cyclohexane have different electrical conductivities. At room temperature, two specific chair isomers with different electrical conductivities can be detected by eliminating noise from the characteristics.[117] The force control change process between the two chair configurations can be monitored by introducing force to regulate the configuration of cycloethane through electrical characteristics (Figure 9d).[118] It is also possible to monitor the structural changes of molecules stretched or folded by force. For example, under the action of force, the molecule unfolds/folds, corresponding to different conductance states. The changes in the molecular structure caused by the force can be monitored using the electrical characteristics of the conductive atomic force microscope.

In addition to the mechanical force regulation, the molecular isomerization regulation based on the electric field force has been effectively monitored. For example, the *cis*−*trans* isomerization of cumene derivatives has been regulated using an electric field force (Figure 9e).[119] First, the molecule is fixed at both ends of the electrodes. The electrical measurement of its *cis* structure revealed that the conductivity histogram changes with time. The peak height of the histogram and length of the conductance platform increases with time. The conductivity characteristics are similar to those of the molecular *trans* structure after approximately 32 h. However, there is no corresponding change in the measurement of the conductivity of the molecular *trans* structure. The comparison experiment with a catalytic environment without STM-BJ, using high-performance liquid chromatography and theoretical calculation, shows that the process of molecular isomerization is successfully monitored using the STM-BJ technology, that is, the *cis* structure of the molecule changes to the *trans* structure. Simultaneously, it explains how the directional electric field formed between the tip and the substrate induces the change in the *cis*−*trans* isomerization process.

Similarly, the monitoring of the force-controlled isomerization process of tetramethyl carotene can also be realized using dynamic and static STM methods to characterize the molecular conductance (Figure 9f).[120] Two more discrete conductance signals can be obtained by applying different high and low bias voltages. Theoretical calculations show that the overall conductance of the *cis* carotenoid monolayer junction is controlled by the gauche defect, which disrupts the π-orbital electron path through the molecules, resulting in lower conductance. Therefore, the two conductance states can be attributed to the *cis* and *trans* isomers of carotenoids. Furthermore, the calculation of the electronic structure shows that the excited states are mixed because of the polarization of molecules by an electric field. Because there is a permissible transition process in the mixed excited states, this process could not only promote the *cis* isomerization of molecules but also participate in electron transfer.

MONITORING OF INTERMOLECULAR INTERACTIONS

The intermolecular interaction is the basis for the formation and evolution of matter. The monitoring of intermolecular interaction and its dynamic change process has been realized because of the ultrahigh temporal and spatial resolution of single-molecule junction technology. This section introduces some important developments in the monitoring of intermolecular interactions, such as hydrogen-bond interactions between simple molecules, host−guest interactions between complex molecules, and interactions between biological macromolecules.

Hydrogen-Bond Interaction. A hydrogen bond is an important component of intermolecular interactions. Hydrogen atoms with a small size can enhance the interaction of dipole or charge through electrostatic interaction between molecules, to form hydrogen bonds between molecules.[121−123] Using a molecular probe to quantify the electron-transfer process through the hydrogen bond between single molecules is an effective method to understand electron transport at the single-molecule level. Through the STM-BJ technology, the tip of STM molecules modified by ω-carboxyl alkanethiols was

https://doi.org/10.1021/acsnano.1c11433
ACS Nano XXXX, XXX, XXX−XXX

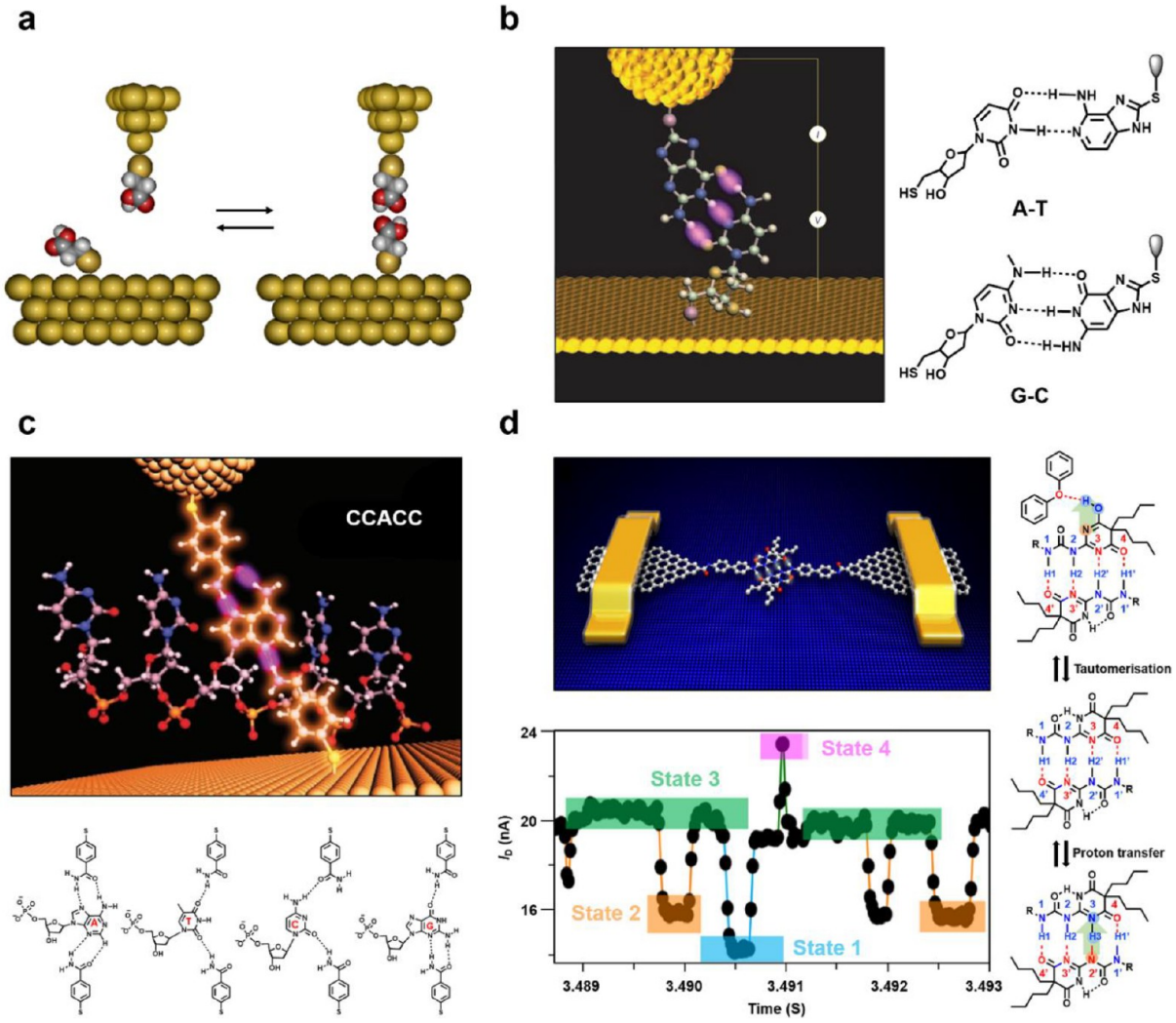

Figure 10. (a) Schematic of tunneling current measurement setup and procedure. The electron transfer through a hydrogen bond was measured via spontaneous formation of a chemical interaction between the tip and sample molecules. Reprinted with permission from ref 124. Copyright 2013 American Chemical Society. (b) Illustration of hydrogen-bonded interactions of the STM measurements and structure of molecular interaction (right). Reprinted with permission from ref 126. Copyright 2009 Springer Nature. (c) Schematic of benzamide groups on the probe and substrate bonded bases in the polymer (highlighted for the connection to the single A in d(CCACC)) and hydrogen-bond formation structures of four different bases. Reprinted with permission from ref 127. Copyright 2010 Springer Nature. (d) Device structure and electrical characterization of HBB-SMJs. *I*–*t* curves of an HBB-SMJ device in diphenyl ether at 323 K and the molecular structures corresponding to different conductance states (right). Reprinted with permission under a Creative Commons CC-BY license from ref 128. Copyright 2018 Springer Nature.

close to the gold substrate modified by C_nCOOH, and the current between them was measured (Figure 10a).[124] Because carboxylic acids are prone to hydrogen-bond interactions in nonpolar solvents, electron transfer of hydrogen bonds is through the intermolecular interaction between tip and sample molecules. Particularly, hydrogen-bonded molecular junctions have higher conductance than covalent σ bonded junctions. The electron-transfer characteristics through hydrogen bonds depend significantly on length, indicating that the electrical connection between single molecules can be deliberately controlled by adjusting the length of hydrogen-bond connectors.[125] For instance, DNA base pairs were used to functionalize STM probes. In 1,2,4-trichlorobenzene solution, the gold substrate contact of a modified nucleoside monolayer was used to measure the strength of hydrogen bonds in DNA-base pairs (Figure 10b).[126] The results show that the signal attenuation connected by three hydrogen bonds (guanine deoxycytidine, G-C and 2-aminoadenine thymidine, 2AA-T) is slower than that connected by two hydrogen bonds (adenine thymidine, A-T and 2-aminoadenine deoxycytidine, 2AA-C) by measuring the current between different base pairs. Furthermore, the rigidity of hydrogen bonds in minor molecular interactions can be characterized using STM.

Furthermore, hydrogen bond plays a universal role in molecular recognition. For example, 4-mercaptobenzamide is used to chemically modify a gold electrode and substrate, in which a mercapto group is connected to the electrode, and the function of the amide bond is similar to that of the probe (Figure 10c).[127] The target molecule (DNA oligomer or amino acid) can be captured between the electrodes to generate a tunneling current through the interaction of intermolecular hydrogen bonds, which can be used to construct a single-

https://doi.org/10.1021/acsnano.1c11433
ACS Nano XXXX, XXX, XXX–XXX

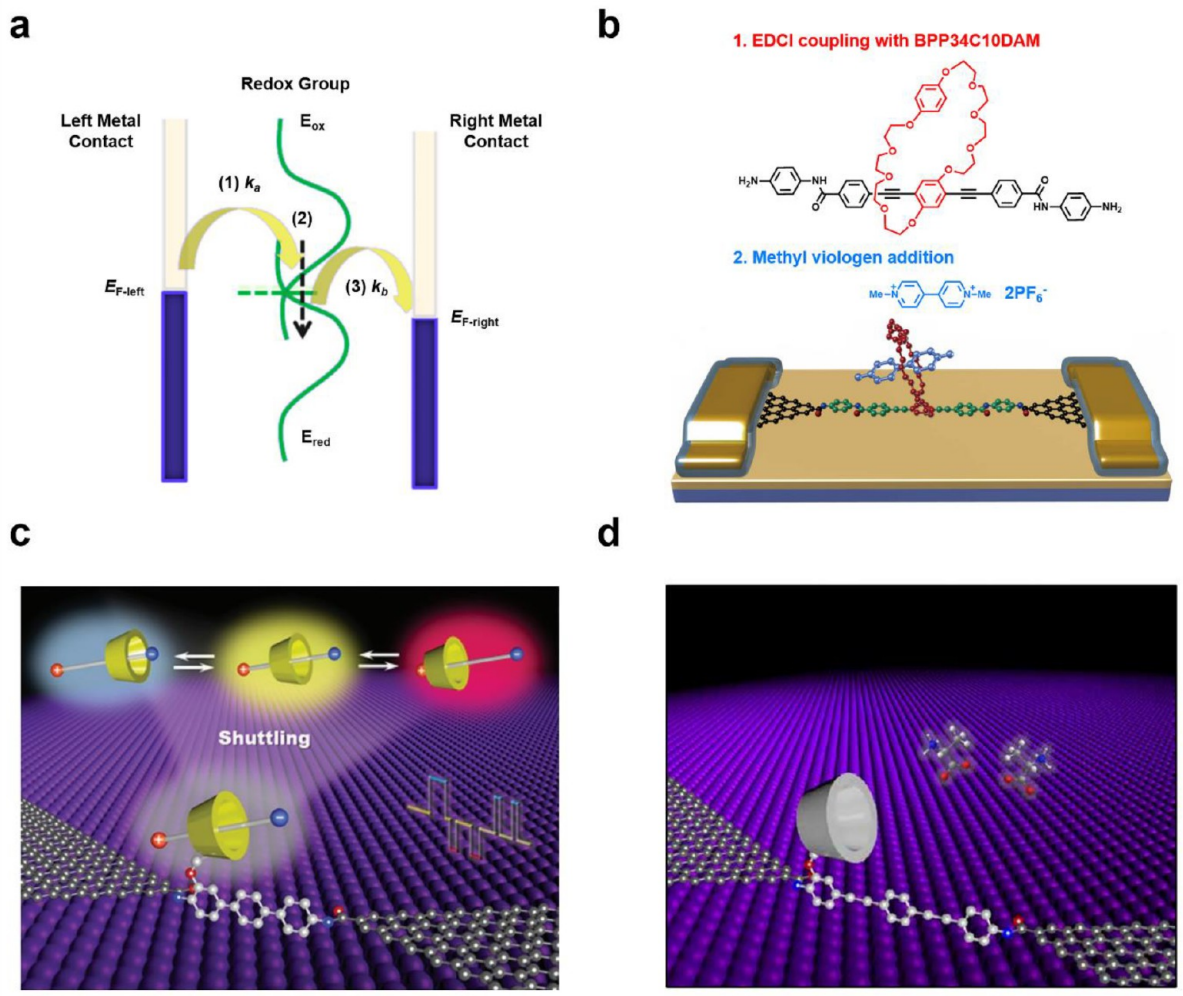

Figure 11. (a) Scheme of a viologen-cucurbituril[8] molecular junction. Reprinted with permission from ref 139. Copyright 2016 American Chemical Society. (b) Schematic representation of the MV^{2+}⊂BPP34C10-SMJ, host molecular structure (black) and guest molecular structure (blue). Reproduced from ref 140. Copyright 2016 The Authors, some rights reserved; exclusive licensee AAAS. Distributed under a CC BY-NC 4.0 license. (c) Schematic representation of the device structure of GMG-SMJs formed from individual molecular shuttles. Reprinted with permission from ref 142. Copyright 2019 Wiley-VCH. (d) Schematic representation of a PM-β-CD-based GMG-SMJs. The molecular machine featuring a PM-β-CD was covalently connected with graphene point contacts through amide bonds. Reproduced from ref 143. Copyright 2021 The Authors, some rights reserved; exclusive licensee AAAS. Distributed under a CC BY-NC 4.0 license.

molecule electric detector. By training the algorithm on single-component samples of all amino acids, the specific amino acids in the mixture can be identified, including chiral enantiomers, isomers, and methylated variants.

Furthermore, the hydrogen bond exists as a special chemical bond, which can participate in various chemical reactions, such as bond rearrangement, proton transfer, as well as catalysis. Therefore, the study of hydrogen-bond dynamics at the single-molecule level is critical. A quadruple hydrogen-bond dimer based on urea pyrimidine dione (Upy) is covalently connected to graphene electrodes as a molecular bridge (Figure 10d).[128] Upy dimer molecules form an intermolecular tetrahydrogen-bond-donor receptor array, which can stably monitor the dynamic behavior of hydrogen bonds in real time for a long time. Additionally, molecules can only form a single double chain because of the main influence of degeneracy, which simplifies the research object.[129] Furthermore, Upy dimer molecules can form or dissociate in diphenyl ether or water. Different conductance states can be monitored by alternating testing of diphenyl ether and water. In addition, this study also shows that the influence of the external testing environment on the hydrogen-bonding system can also be well observed by single-molecule devices. State 4 exhibits a spike-like high-frequency signature with an extremely short lifetime, indicating that the nonsteady-state distribution broadens with increasing temperature. These features indicate transient perturbations in the quadripolar hydrogen-bonding system, which is a common phenomenon in single-molecule/single-event measurements. Therefore, state 4 is presumed to be a stable state caused by the binding of diphenyl ether molecules to molecular reactive sites to weaken hydrogen bonds.

Host–Guest Interaction. Host–guest interaction is an important part of chemical research. Using host–guest interaction to identify chemical and biomolecules is an important research direction in the field of science and the cornerstone for understanding the mechanism of chemical interactions and the essence of biological functions.[130−133] Single-molecule junction technology, as a reliable monitoring platform at the single-molecule level, is an effective method for revealing interaction mechanisms.

https://doi.org/10.1021/acsnano.1c11433
ACS Nano XXXX, XXX, XXX−XXX

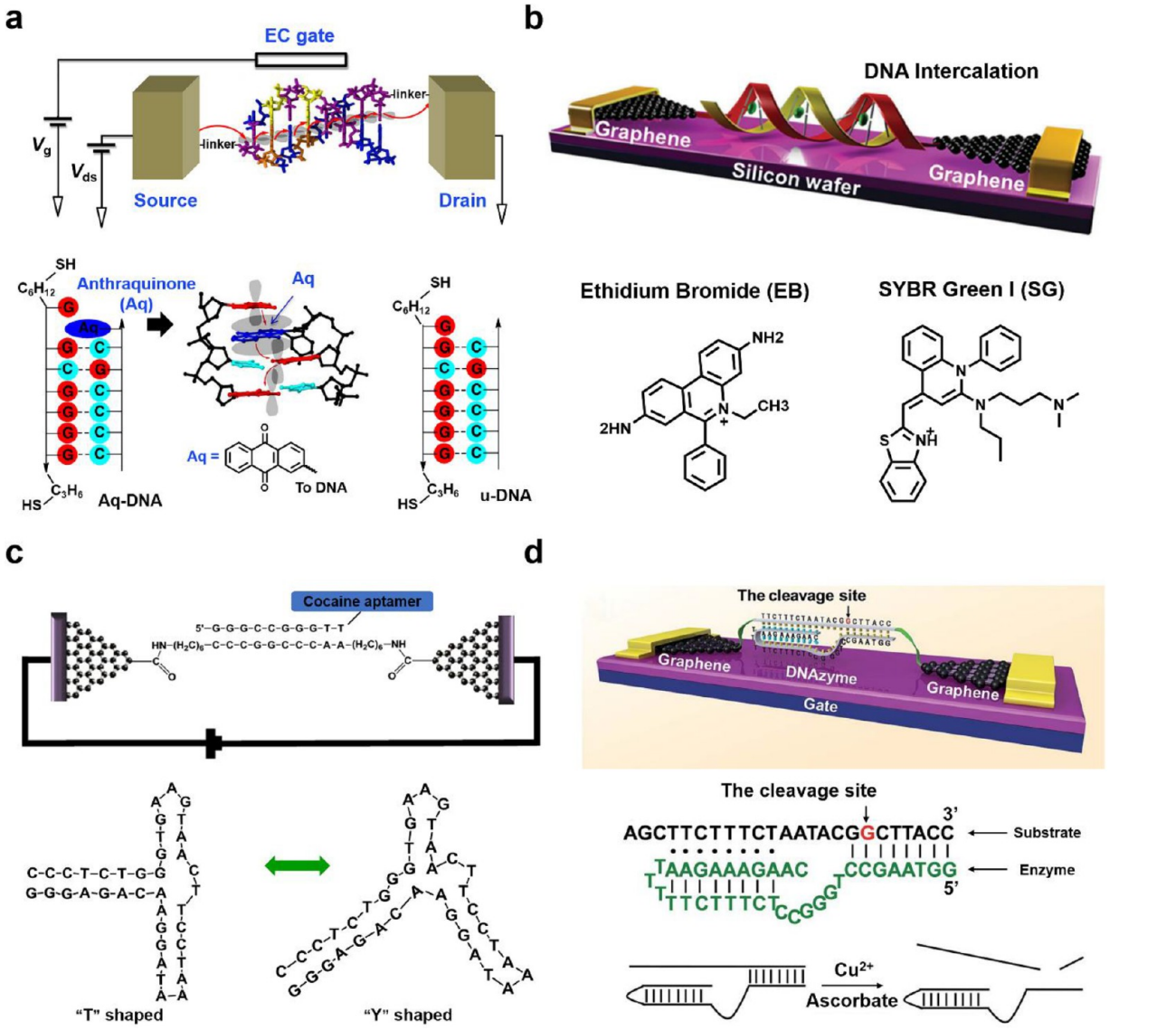

Figure 12. (a) Illustration of the experiments, where source and drain electrodes are the STM tip and substrate, and the EC gate is a silver electrode inserted in the solution. From left to right: DNA was modified with AQ DNA (Aq-DNA) (AQ partially highlighted in blue). The Aq part between two guanine bases on the other chain serves as a jumping site for electron transfer (red arrow). The end is terminated with a vulcanized connector for contact with source and drain electrodes. Reprinted with permission under a Creative Commons CC-BY license from ref 154. Copyright 2017 Springer Nature. (b) Schematic representation of DNA-functionalized molecular junctions, and the molecular structures of EB and SG. Reprinted with permission from ref 155. Copyright 2015 Royal Society of Chemistry. (c) Schematic representation of the device structure and the structural changes after aptamer binding to cocaine. Reprinted with permission from ref 156. Copyright 2019 Wiley-VCH. (d) Schematic representation of graphene-DNAzyme junctions, and the structure of the Cu^{2+}-sensitive DNAzyme and corresponding catalytic activity. The cleavage site is indicated by an arrow. Reprinted with permission under a Creative Commons Attribution 3.0 Unported License from ref 158. Copyright 2015 Royal Society of Chemistry.

For example, cucurbituril is a macrocyclic molecule formed by the condensation of glycosuria and formaldehyde under acidic conditions. The glycosuria units are bridged together by methylene, with hydrophilic carbonyl groups at both ends and hydrophobic cavities in the middle. Cucurbituril has a strong inclusion ability for positively charged guest molecules such as protonated organic amines, pyridinium, as well as viologen.[134−136] Among them, viologen molecules have reversible redox discoloration, and the inclusion of cucurbituril has good stability to viologen reduced free radicals. Therefore, the study of viologen/cucurbituril composite systems in the fields of stimulus-responsive materials and supramolecular self-assembly has attracted much attention.[137,138]

Specifically, the host−guest interaction between cucurbit[8]-uril and viologen molecular bridges are used to construct four different molecular wires, which are connected to a single molecular circuit using MCBJs for electrical testing (Figure 11a).[139] The characterization results show that the conductance of viologen derivatives increases significantly when encapsulated in the hydrophobic cavity, which is because of the reduction of an outer sphere recombination energy within the framework of the Marcus-type electron-transfer model.

Similarly, host−guest interaction can monitor rich changes in molecular conductance signals. For instance, the two ends of the molecular bridge of crown ether derivatives are covalently linked into graphene electrodes to construct the GMG-SMJ

https://doi.org/10.1021/acsnano.1c11433
ACS Nano XXXX, XXX, XXX−XXX

molecular device (Figure 11b).[140] Methyl viologen was introduced as a guest molecule in the electrical testing process, and the dynamic process of the molecular host−guest interaction can be directly observed. The regular fluctuation of molecular conductance can be attributed to the generation and dissociation of host−guest complexes. Furthermore, the charge variation during the host−guest interaction can be used as an additional local gate to adjust the carrier density in the conductive channel because the molecular bridge is similar to the traditional field-effect transistor, resulting in a significant change in molecular conductance.

For example, the conductance of molecular wires through the complexation between the guest and host can be regulated by the host using a single cyclodextrin molecule junction device with graphene electrodes.[141] Specifically, dimethyl α-cyclodextrin (PM-α-CD) and charged alkylene axis can form pseudorotaxane structures through intermolecular interaction (Figure 11c).[142] By using the charge of the alkylene axis, not only the complex can be stably formed but also the shuttle process of guest molecules can be monitored in real-time based on the distance of the potential point. Therefore, when dodecanedioic acid is used as a negative charge to fill the guest in the hole, the perturbed-HOMO (p-HOMO) of pseudorotaxane is close to the Fermi level of the electrode, improving the molecular conductance. However, when 1,12-dodecanediamine is selected as the positively charged guest to fill the hole, p-HOMO of pseudorotaxane will be far from the Fermi level of the electrode, which helps reduce the conductance. A mutual jump of conductance states was observed for zwitterionic 12-aminododecanoic acid when the negative and positive charges of the molecule are filled alternately by the cyclodextrin molecule.

In a word, the host−guest interaction can detect not only the formation of molecular complexes but also the interaction process. These refined data can lay a solid foundation for molecular recognition. Additionally, when the main part of the molecular bridge is replaced by dimethylation-β-cyclodextrin (PM-β-CD), using the specific host−guest interaction between β-cyclodextrin and different chiral amino acids can prepare single-molecule detection devices for molecular recognition (Figure 11d).[143] Four amino acids and their corresponding enantiomers were monitored at different pH values. Different host−guest interactions can produce different multimode current fluctuations. By comparing the conductance and kinetic statistics of different enantiomers, the "fingerprint database" of each amino acid can be established.

Interaction with Biological Macromolecules. Biomolecules are an important bridge linking chemistry and life. They have complex and important functions in life. After decades of study, the basic structure of numerous biomolecules has been determined.[144−147] However, analyzing the dynamic reaction process of molecules from a single biomolecule will provide a more accurate and systematic understanding of biomolecule behavior as well as a deeper understanding of biomolecule functions in organisms.[28,148,149] The single-molecule junction technology provides an effective method to realize this concept. Monitoring the complex interactions of biological systems at the molecular level provides a significant opportunity to reveal the details of the basic process of life.

DNA, as an important biological macromolecule, plays a significant role in the life system. It has specific conductance characteristics that can be monitored by single-molecule junctions because of its structure, which is the complementary pairing of the double helix structure and base.[150−153] For example, using the interaction between bases in DNA molecules, a base is replaced with anthraquinone (AQ), and then DNA molecules are chemically modified on gold substrates (Figure 12a).[154] In the absence of a gate electrode, AQ DNA has good conductivity because the molecular orbital of AQ overlaps with the orbital of adjacent bases, forming a continuous $\pi-\pi$ stacking path along DNA that can realize effective charge transfer. Furthermore, because AQ is a reversible redox group in the gate electrode, switching between two different high and low conductance states can be measured by switching the state between oxidation and reduction.

The DNA sensor based on GMG-SMJs also performs well in detecting the interaction between DNA and other molecules (Figure 12b).[155] For instance, two different intercalators (ethidium bromide (EB) and SYBR Green I (SG)) were added to the solution for electrical measurement. The limit of detection was significantly reduced through the measurement of different concentrations because of its available covalent link mode (approximately 5.0×10^{-13} mol·L^{-1} for EB and approximately 2.0×10^{-14} mol·L^{-1} for SG), which had a good signal-to-noise ratio while detecting the change of the DNA conductivity.

Single-molecule devices can detect not only the interaction between biological macromolecules and chemical small molecules but also the interaction between biological macromolecules. Through detecting the corresponding conductance changes caused by conformational changes during biomolecular interactions, molecular characteristics can be obtained more conveniently and quickly. Meanwhile, this type of single-molecule biosensor is more sensitive and accurate. For example, cocaine aptamer, a chain of double-stranded DNA with complementary cocaine aptamer sequences, is coupled to the molecular bridge as a side chain molecule, and the molecular bridge is fixed at both ends of graphene electrodes through amide bonds (Figure 12c).[156] The conformational changes of aptamer binding with cocaine can be measured using electricity because the binding of cocaine changes the tertiary structure to a state with higher conductance, and the corresponding current changes can be obtained.

Furthermore, a low level of free metal ions in organisms is critical for the healthy growth and continuation of life.[157] Monitoring the interaction between biological macromolecules and metal ions using single-molecule junction technology is critical for understanding the role of interaction in biology. DNAzymes were combined with GMG-SMJs to achieve this (Figure 12d).[158] DNAzymes, as a type of DNA biocatalyst, can interact with metal ions. Its conductivity gradually decreased to zero, indicating that the interaction between DNAzymes and copper ions resulted in the breakage of DNAzymes caused by the conformational change.

MONITORING OF CHEMICAL REACTIONS

Monitoring chemical reactions at a single-molecule level can reveal the basic laws of chemical reactions hidden in ensemble experiments. Additionally, the impact of the microenvironment on chemical reactions can be effectively explored in single-molecule experiments. Precise control of the chemical reaction process at the single-molecule level is critical for guiding the design of chemical reactions. This section introduces the monitoring of chemical reaction paths with single-molecule junctions, including the capturing of intermediates produced

https://doi.org/10.1021/acsnano.1c11433
ACS Nano XXXX, XXX, XXX−XXX

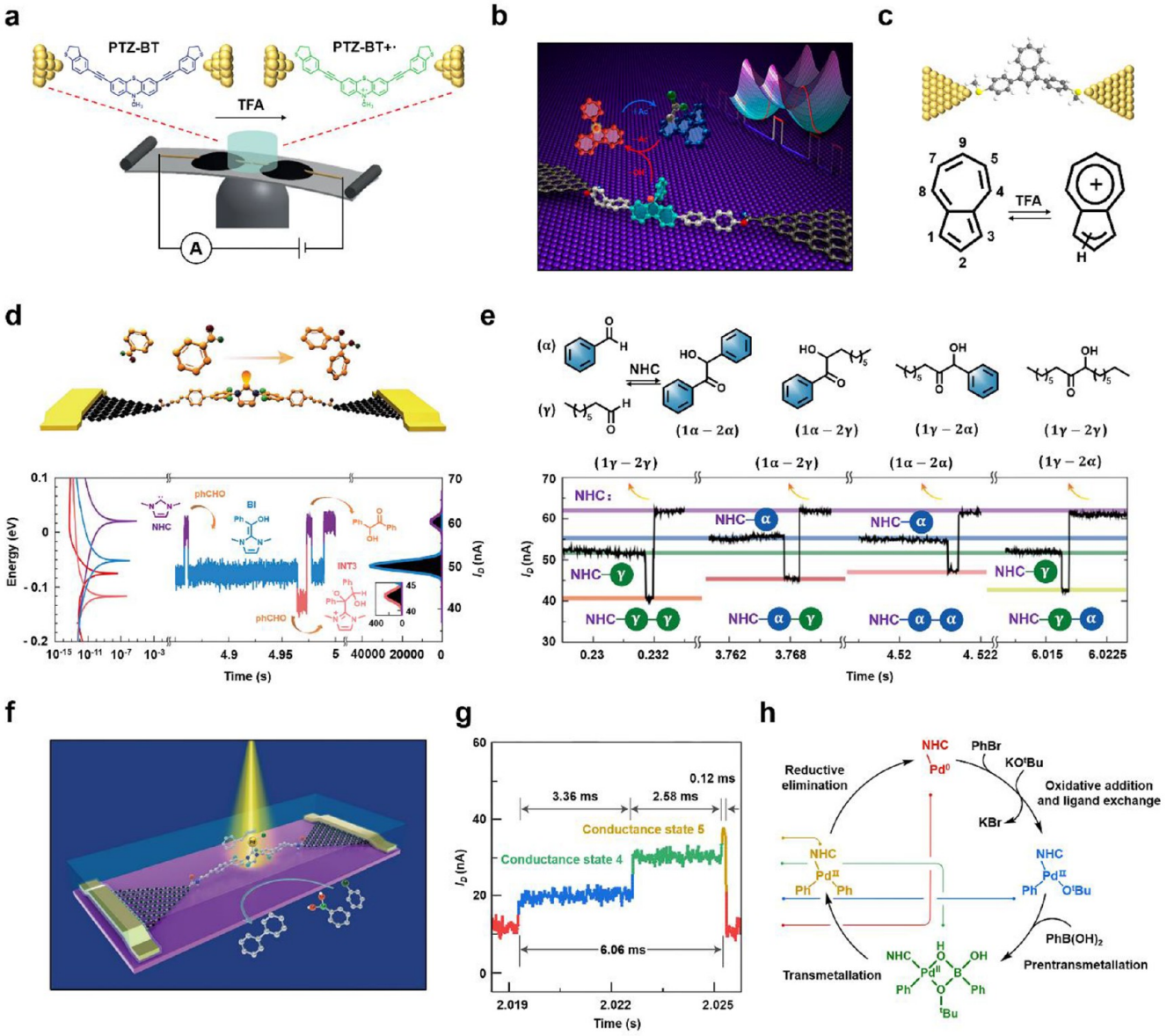

Figure 13. (a) Schematic of the MCBJ setup and radical generation of a PTZ derivative. Reprinted with permission from ref 164. Copyright 2017 Wiley-VCH. (b) Schematic of a GMG-SMJs that shows the path of transformation of a 9-phenyl-9-fluorenyl cation in an S_N1 reaction. Reprinted with permission from ref 23. Copyright 2018 American Chemical Society. (c) Schematic of a MCBJ-based molecular junction of 1,3 azulene and its protonation process after adding TFA. Reprinted with permission under a Creative Commons Attribution 3.0 Unported License from ref 165. Copyright 2017 Royal Society of Chemistry. (d) Schematic diagram of the single-molecule electrical monitoring device and real-time electrical spectroscopy of benzoin homocondensation. Left: Transmission spectra of four species. Center: Real-time electrical spectroscopy of benzaldehyde condensation. Right: Corresponding statistical histograms. (e) Schematic diagram of benzoin cross-condensation and its real-time electrical spectroscopy. Reprinted with permission from ref 166. Copyright 2021 Elsevier Inc. (f) Illustration of a single-molecule catalytic device. (g) One catalytic cycle showing four conductance states. (h) Molecular structures and reaction paths of Suzuki−Miyaura cross-coupling. Reprinted with permission from ref 27. Copyright 2021 Springer Nature.

during reaction and regulation of chemical reactions through electric fields.

Capturing of Active Intermediates. Many chemical reactions are complex, consisting of elementary reactions, in which at least one active intermediate is formed. The study of their production, structure, and change can help reveal the reaction process and guide organic synthesis. However, these active intermediates have a short life and are difficult to separate. The single-molecule junction, as a generic electrical detection method, can provide a reliable and promising method for detecting intermediates in the chemical reaction process.

Free radicals, as one of the active intermediates of chemical reactions, play a critical role in various chemical reactions. Therefore, the detection of free radicals is also an important direction in chemistry. Because free radicals are atoms or groups with unpaired electrons formed by homogeneous cleavage of covalent bonds, most free radicals have high chemical activity. However, free radicals with high chemical activity lack stability and are difficult to be monitored directly.[159−162]

https://doi.org/10.1021/acsnano.1c11433
ACS Nano XXXX, XXX, XXX−XXX

The emergence of single-molecule junction platforms can help solve this challenge. The emergence of active free radicals can be easily captured using electrical monitoring technology with high temporal and spatial resolution. Phenothiazine (PTZ) molecules can use trifluoroacetic acid (TFA) as an oxidant to conduct one-electron oxidation on the nitrogen atom in the molecule to form free radical cations.[163] When the free radical is formed using the MCBJ technology to construct a single-molecule junction with PTZ as the core, the conductivity of the free radical is significantly higher than that of the molecule because the HOMO−LUMO gap is significantly reduced and the transmission near the HOMO orbit is enhanced (Figure 13a).[164]

Improving the temporal resolution of electrical detection allows monitoring of reaction intermediates. Specifically, graphene electrode-based single-molecule junctions connect single molecules into devices via stable amide covalent bonds, which can be used to study single molecular chemical reactions in situ. Through the time-dependent current signal, the chemical reaction process can be effectively revealed. By improving the sampling frequency of the monitoring instrument, the information of the intermediates and their lifetime evolution paths at corresponding time scales can be obtained. For example, the presence of carbocation intermediates can be monitored by the GMG-SMJ platform at a sampling frequency of 57.6 kHz (Figure 13b).[23] The results show that the carbon cation intermediate can be effectively captured in the mixed solution of trifluoroacetic and acetic acids. Because the structure of the carbon-positive ion is sp^2 coplanar, its conductance is significantly higher than that of the acetate species, and there is a transformation between them. Furthermore, introducing bromine ions into the testing environment can monitor the competitive transformation between acetic acid and bromine species in real-time. The transformation between the two substances inevitably goes through carbon cation intermediates, which confirms the classical S_N1 reaction mechanism.

Protonation is not only a basic chemical reaction but also an important step in many stoichiometric and catalytic processes. Similarly, protonated products participate in many important chemical reactions as an important intermediate. Five seven-ring systems of azulene derivatives (AZ) can be protonated in an acidic environment, and its protonated products can be captured by the MCBJ method (Figure 13c).[165] The conductivity after protonation is significantly improved compared with that before protonation because the HOMO and unpaired valence electrons of the protonated azulene nucleus move toward the Fermi level of the electrode. Furthermore, the positions of different anchoring groups in a molecular skeleton can significantly impact the electrical transport properties of the molecule. By using the single-molecule circuit constructed by 5,7-AZ as an example, the conductance can significantly change after protonation. The reason is that the neutral 5,7-AZ molecule has interference near the Fermi energy. Protonation destroys this interference, making the conductance change significantly.

After years of innovation and development, single-molecule devices now not only provide an effective platform for capturing intermediates but also provide real-time monitoring of intermediates and reaction steps in the entire chemical reaction, especially for the graphene electrode system. The single-molecule device constructed by covalent bonding of molecules ensures the stability and high signal-to-noise ratio of molecular testing, and the transformation path between intermediates in the reaction path can be monitored more intuitively through electrical monitoring method with high time resolution.

Therefore, in addition to the visual reaction path of time series provided by electrical real-time detection, more complex reaction systems can be monitored by single-molecule electrical measurements. For example, azacarbene (NHC) with a catalytic function can be connected to single-molecule devices as a functional center. The cross condensation of a benzoin reaction was studied (Figure 13d).[166] First, by introducing benzaldehyde into the reaction system, two intermediates, enol Breslow intermediate (BI) and readdition intermediate (INT3), can be captured. Furthermore, after reducing the test ambient temperature, the first addition intermediate (pre-BI) can be captured. Additionally, as more octanal is introduced into the system, the current state increases to seven conductance states, including two intermediates (NHC) catalyzed by NHC-α and NHC-γ. The conductivity states of the intermediates of cross condensation between the two intermediates and secondary addition of the intermediates can also be detected (NHC-$\alpha-\gamma$, NHC-$\gamma-\alpha$, NHC-$\alpha-\alpha$, and NHC-$\gamma-\gamma$) by adjusting the state of the NHC catalyst (Figure 13e). The distribution of these conductivity states is due to the powerful electrical real-time monitoring of single-molecule devices. Species monitoring based on this time sequence can intuitively allocate species in complex reaction systems.

As previously stated, this single-molecule device based on covalently bonded graphene has a high device stability and can withstand chemical treatment and external stimulation. Therefore, using NHC as a transition-metal carrier can further study the complex organic chemical reaction catalyzed by transition metals.[167] For instance, in a palladium-catalyzed Suzuki−Miyaura coupling reaction (Figure 13f), by monitoring a catalytic cycle at the junction of a single catalyst, two controversial reaction modes can be distinguished, that is, whether an alkali-activated intermediate complex appears in the catalytic path.[27] According to the time series of the detected species, four intermediates in the catalytic cyclic path can be captured, including Pd(0), oxidative addition/ligand exchange complex, pretransmetalation complex, and transmetalation complex (Figures 13g,h). The correlation between reaction paths in Suzuki−Miyaura coupling can also be directly observed.

Regulation of Chemical Reactions via Electric Fields. Chemical reactions are often accompanied by intermolecular charge transfer. Chemical reactions can be controlled by regulating the charge distribution in the reaction substrate molecules.[168−170] An effective regulation method is to use an electric field applied at both ends of the electrodes in a single-molecule device. The electric field acting on the molecule on both sides of the electrodes can increase significantly as the distance between the electrodes decreases, and the nanoscale electrode will produce a strong electric field in the single-molecule device.

Diels−Alder reaction is a chemical reaction between conjugated dienes and dienes, which is widely used in the field of organic synthesis and biochemistry.[171,172] Particularly, the process of the Diels−Alder reaction can be regulated by an external electric field. Specifically, the directional external electric field can control the Diels−Alder reaction rate and its internal/external selectivity.[173]

https://doi.org/10.1021/acsnano.1c11433
ACS Nano XXXX, XXX, XXX−XXX

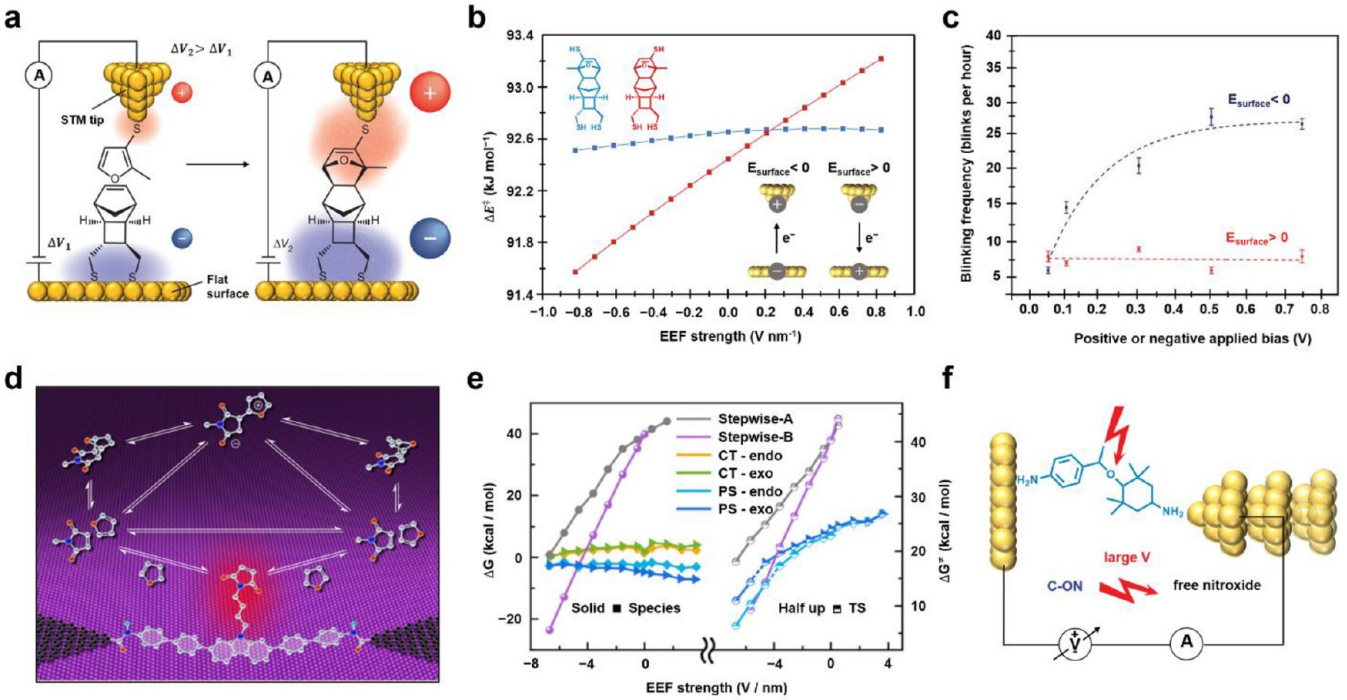

Figure 14. (a) Schematic of a STM-BJ measurement setup and procedure. The diene (a furan) is attached to the STM tip via a thiol group ('S'); the dienophile (a norbornylogous bridge) is attached in a known orientation to a flat gold surface via two thiols. (b) The predicted effects of the strength and direction of the external electric field on the reaction-barrier height ($\Delta E^{\ddagger}$) for the formation of the two *exo*−*syn* diastereoisomers. The two intermediates have different responses to electric fields, and the blue molecular structure has more obvious electric field dependence than the red molecular structure. The direction of the electric field is shown in the figure at the bottom right corner. (c) Blinking frequency as a function of applied bias. Positive and negative biases are plotted in red and blue, respectively. Reprinted with permission from ref 25. Copyright 2016 Springer Nature. (d) Schematic diagram of another single-molecule electrical monitoring platform and mechanism of the Diels−Alder reaction. (e) Quantitative analysis of the EEF effect. The Gibbs free energy of each species and transition state increases with the increase of the electric field intensity. Reprinted from ref 26. Copyright 2021 The Authors, some rights reserved; exclusive licensee AAAS. Distributed under a CC BY-NC 4.0 license. (f) Illustration of a STM-BJ device and C-ON bond breaking mechanism. Red lightning indicates the location of the broken bond and the factors that cause the breakage. Reprinted with permission from ref 176. Copyright 2018 American Chemical Society.

Recently, studies on the single-molecule Diels−Alder reaction have consistently demonstrated that the electric field can regulate the reaction. For example, a furan derivative as the diene and a norbornylogous bridge with a terminal double bond as a nonpolar dienophile are connected to an STM tip and a flat gold surface, respectively (Figure 14a).[25] The STM structure is used to realize directional external electric fields. Therefore, the Diels−Alder reaction is controlled by junction bias. If the Diels−Alder reaction between conjugated dienes and dienophiles occurs when the needle tip contacts the substrate surface, there will be a sudden change in current. When the electron flow direction is along the bottom of the needle tip, the probability of detecting reaction products is significantly higher, which is positively correlated with the applied bias voltage (Figure 14b). However, when a reverse electric field is applied, the probability of the product occurrence decreases and does not correlate with the field strength. This conformation has the lowest potential barrier in the presence of a specific electric field because dienes are rich in electrons, whereas amphiphilic compounds lack electrons. Furthermore, through a STM break junction experiment called "blinking", in the case of the negative bias, the Diels−Alder reaction is monitored more times with increasing biases, indicating that the energy barrier of the reaction process is lowered by the electric field (Figure 14c). Therefore, the reaction pathway is regulated through a directional external electric field.

For example, compound **a** (3,6-bis(4-pyridyl)1,2,4,5-tetrazine) reacts with dihydrofuran through an inverse electron demand Diels−Alder reaction to produce **b**, and then **b** aromatizes to produce **c**. The MCBJ technology is used to regulate and monitor the cascade reaction with a directional external electric field.[174] In the first step, the external electric field does not produce a catalytic function because the molecular reaction axis is orthogonal to the direction of the external electric field. In the aromatization process of the second step, the reaction axis is not orthogonal to the oriented external electric fields in the single-molecule junction, so the electric field accelerates the reaction rate of the second step.

The strong electric field provided between nanoelectrodes can not only regulate the reaction path but also obtain and stabilize reaction intermediates to produce interrelated reaction paths. Taking the Diels−Alder reaction as an example, it is usually a synergistic reaction, but the definition of the reaction mechanism is often limited by the time limit of instrument monitoring. By using in situ monitoring means of high stability and time resolution of GMG-SMJs, the mechanism of the Diels−Alder reaction can be more comprehensively analyzed (Figure 14d).[26] A zwitterionic intermediate can be observed as temperature increases. In addition to the corresponding two products, the generation of

https://doi.org/10.1021/acsnano.1c11433
ACS Nano XXXX, XXX, XXX−XXX

extra intermediates increases as the electric field increases, and the intermediates can be stabilized as the electric field increases (Figure 14e). Note that a random optical reconstruction microscope is also used to synchronize the strong correlation experiment with an electrical signal, which demonstrates the capability of using the GMG-SMJ platform to monitor reaction processes.

The effect of external electric fields can affect the chemical reaction from both positive and negative aspects and can reduce or increase the reaction barrier, which means that through careful design, the external electric field can regulate the formation and fracture of chemical bonds.[175] For example, the electric field carried by functional groups with negative charges at the distal end can promote the homolysis of alkoxyamine molecules at lower temperatures by electrostatic interaction, which means that the entire process can be monitored by electrical signal measurements. Specifically, alkoxyamines were grafted by a monolayer chemical method with STM-BJ (Figure 14f). Therefore, the reactants were aligned with double layers of the electrochemical cell.[176] The C-ON chemical bond can be dissociated under the action of an electric field to form carbon radical and corresponding nitrogen oxide. Under electrochemical conditions, positive carbon ions and corresponding nitrogen oxides were formed by bonding. Even in the electrochemical process, the C-ON cracking step can only be realized by electrostatic interaction.

CONCLUSIONS AND OUTLOOK

Single-molecule devices show possibilities for various potential applications, especially in the study of physical and chemical processes.[177,178] This study summarizes important recent works in physics and chemistry from the viewpoint of monitoring molecular charge transport using single-molecule junction technologies. First, the monitoring of charge transport characteristics and quantum behavior of single molecules under gate electric and magnetic fields is introduced. We focus on the regulation of single-molecule charge transport through different types of gating and various regulation of the spin states of single molecules. Then, the monitoring of single-molecule isomerization processes under various stimuli, such as temperature, light, electricity, and force, is introduced. Exploration of intermolecular interactions is also discussed, such as hydrogen bonds, host−guest, and biological macromolecular interactions. Finally, significant applications of single-molecule junctions in the field of exploring single-molecule chemical reactions are highlighted, such as capturing reaction intermediates, monitoring reaction paths, and regulating reaction processes. Furthermore, the current fabrication techniques of single-molecule junctions and molecular connection methods are summarized and compared (Tables 1 and 2). On this basis, many inherent and important phenomena can be discovered by studying the basic mechanisms of single-molecule physics and chemistry. However, more sensitive and efficient single-molecule functional devices can be realized using the physical properties of molecules and the state control of chemical reactions.

However, the study on the physical or chemical processes of single molecules, especially related research on the internal mechanism and regulation of state transition, remains insufficient. There are still many challenges in the improvement of the monitoring technology, expansion of the research system, and extensive application of research results.

First, accurately monitoring and controlling the charge state of single molecules is one of the main challenges. Specifically, the internal mechanism of gate regulation is to adjust the molecular potential energy by applying a gate electric field, controlling the relative energy difference between the molecular orbital and the Fermi level of the electrode. Although the liquid gate can give powerful adjustment capabilities through the electric double layer, the inherent properties of the liquid-gate limit the development of molecular device integration. The solid gate with environmental stability and high controllable regulation ability is more in line with the development direction of molecular electronics. Therefore, it is critical to develop late-model solid gate control methods to effectively apply gate field to single molecules. Additionally, the developed solid-state gate electrodes should work stably in various environments, so powerful regulation methods can be better integrated into research strategies, such as ultralow temperature, strong magnetic field, strong electric field, as well as a light field. Therefore, the quantum state laws and effects of single molecules can be studied in depth. Especially, the electrons on single molecules can be accurately controlled using these methods, which is helpful to further study the electrocatalytic mechanism of chemical reactions.

Second, there are still some challenges in monitoring the structural changes of single molecules. The isomerization process of single molecules has been effectively monitored by single-molecule junctions. Simultaneously, various methods have been developed to control molecular isomerization, including light, electricity, force, and chemical stimuli. Although various control methods have been developed and applied, how to accurately monitor the isomerization process of single molecules at the single chemical bond level remains a challenge, such as real-time monitoring of the photoexcitation process, the chemical bond rotation process, and the use of force to precisely control chemical bonds. Because the time scale of the isomerization is usually in the femtosecond range, process exploration is usually limited using monitoring time resolution, so multimode strategies should be developed in conjunction with femtosecond optics. Emerging stimulation methods must be introduced, including polarized light, terahertz, infrared, and others. Other control technologies, such as optical and magnetic tweezers, should be combined with single-molecule junctions. Additionally, the study of molecular structure changes through single-molecule junctions can be extended to folding/unfolding processes of biological macromolecules, such as DNA and proteins.

Third, consideration should be given to expanding research on monitoring single-molecule chemical reactions. Not only can the path of the chemical reaction be monitored but also the intermediate state during the reaction can be captured using single-molecule electrical characterization technologies. Furthermore, the GMG-SMJs in situ real-time monitoring technology can dynamically monitor the kinetic behavior of single-molecule reactions. The research that has been achieved so far is the capture of reaction intermediates and the monitoring of reaction pathways on time scales above the microsecond level. However, single-molecule junction-based electrical monitoring has not yet achieved the measurement of reaction kinetic processes at the nanosecond or even picosecond scale. In view of this challenge, it is necessary to develop faster electrical testing technology to improve the temporal resolution of electrical monitoring. Furthermore, there is an urgent need to expand single-molecule monitoring

https://doi.org/10.1021/acsnano.1c11433
ACS Nano XXXX, XXX, XXX−XXX

platforms with multiple ultrafast detection methods, such as the introduction of the femtosecond laser technique. Multidimensional molecular information can be obtained through external environmental control and multimode testing methods, which may help meet the needs of ultrafine detection. For instance, femtosecond lasers and strong magnetic fields can be introduced into single-molecule junctions in an ultracold environment to explore single-molecule chemical reactions. Additionally, because most studies on single-molecule junctions are based on electrical monitoring, improving the time resolution and signal-to-noise ratio of electrical monitoring is an important development direction.

Generally, the use of single-molecule devices to monitor single-molecule physical and chemical processes provides the possibility of extraordinary discovering basic physical and chemical laws at the single-molecule level. A variety of single molecule junction technologies and the expansion of different molecular connection methods have been well used to study various physical and chemical properties of single molecules, providing a useful platform for the development of molecular electronics. In addition, the combination of the single molecule junction platform with other test platforms will facilitate further exploration and development of molecular electronics. For example, the combination of optics and electricity can obtain more abundant and multidimensional molecular information by using the information-carrying properties of light itself. Alternatively, the positioning technology of optical tweezers and magnetic tweezers can be introduced to achieve precise control of single molecules. Despite the significant challenges, the extensive research investment in this field can enable physics and chemistry fields to make significant progress at the single-molecule level, allowing them to effectively and accurately manipulate the physical and chemical properties of single molecules. The development of stable multimode regulated single-molecule devices and their corresponding functionalization is highly significant, especially for their extensive applications in organic and biological systems. In addition to the fundamental research, if a good match between the single-molecule junction platform and other monitoring methods can be realized, the technology can realize broad commercial applications with lower power consumption, higher speed, and higher integration.

AUTHOR INFORMATION

Corresponding Authors

Xuefeng Guo − *Center of Single-Molecule Sciences, Institute of Modern Optics, Frontiers Science Center for New Organic Matter, Tianjin Key Laboratory of Micro-scale Optical Information Science and Technology, College of Electronic Information and Optical Engineering, Nankai University, Tianjin 300350, PR China; Beijing National Laboratory for Molecular Sciences, National Biomedical Imaging Center, College of Chemistry and Molecular Engineering, Peking University, Beijing 100871, PR China;* orcid.org/0000-0001-5723-8528; Email: guoxf@pku.edu.cn

Chuancheng Jia − *Center of Single-Molecule Sciences, Institute of Modern Optics, Frontiers Science Center for New Organic Matter, Tianjin Key Laboratory of Micro-scale Optical Information Science and Technology, College of Electronic Information and Optical Engineering, Nankai University, Tianjin 300350, PR China; Beijing National Laboratory for Molecular Sciences, National Biomedical Imaging Center, College of Chemistry and Molecular Engineering, Peking University, Beijing 100871, PR China*; Email: jiacc@nankai.edu.cn

Linghai Xie − *Center for Molecular Systems and Organic Devices (CMSOD), Key Laboratory for Organic Electronics and Information Displays and Institute of Advanced Materials (IAM), Nanjing University of Posts and Telecommunications, Nanjing 210023, PR China;* orcid.org/0000-0001-6294-5833; Email: iamlhxie@njupt.edu.cn

Authors

Xinmiao Xie − *Center for Molecular Systems and Organic Devices (CMSOD), Key Laboratory for Organic Electronics and Information Displays and Institute of Advanced Materials (IAM), Nanjing University of Posts and Telecommunications, Nanjing 210023, PR China*

Peihui Li − *Center of Single-Molecule Sciences, Institute of Modern Optics, Frontiers Science Center for New Organic Matter, Tianjin Key Laboratory of Micro-scale Optical Information Science and Technology, College of Electronic Information and Optical Engineering, Nankai University, Tianjin 300350, PR China*

Yanxia Xu − *Center of Single-Molecule Sciences, Institute of Modern Optics, Frontiers Science Center for New Organic Matter, Tianjin Key Laboratory of Micro-scale Optical Information Science and Technology, College of Electronic Information and Optical Engineering, Nankai University, Tianjin 300350, PR China*

Li Zhou − *Center of Single-Molecule Sciences, Institute of Modern Optics, Frontiers Science Center for New Organic Matter, Tianjin Key Laboratory of Micro-scale Optical Information Science and Technology, College of Electronic Information and Optical Engineering, Nankai University, Tianjin 300350, PR China*

Yong Yan − *Center for Molecular Systems and Organic Devices (CMSOD), Key Laboratory for Organic Electronics and Information Displays and Institute of Advanced Materials (IAM), Nanjing University of Posts and Telecommunications, Nanjing 210023, PR China*

Complete contact information is available at: https://pubs.acs.org/10.1021/acsnano.1c11433

Author Contributions

[§]These authors contributed equally to this work.

Notes

The authors declare no competing financial interest.

ACKNOWLEDGMENTS

We acknowledge primary financial supports from the National Key R&D Program of China (2017YFA0204901, 2021YFA1200101, and 2021YFA1200102), the National Natural Science Foundation of China (22150013, 22173050, 21727806, and 21933001), the Tencent Foundation through the XPLORER PRIZE, "Frontiers Science Center for New Organic Matter" at Nankai University (63181206), the Natural Science Foundation of Beijing (2222009), and Beijing National Laboratory for Molecular Sciences (BNLMS202105).

VOCABULARY

single-molecule junction, single-molecule device is formed by single molecules connected to nanogapped electrodes; high/

https://doi.org/10.1021/acsnano.1c11433
ACS Nano XXXX, XXX, XXX−XXX

low-conductance state, changes in the molecular state will lead to changes in molecular conductance, which can be used for monitoring physical and chemical processes of single molecules; atropisomers, because the rotation around the single bond is hindered, a set of conformational isomers can be separated from each other to form corresponding isomers; carbon electrodes, carbon nanotubes, or graphene are processed from the bottom-up method to form nanogapped electrodes; electronic coupling of the molecule−electrode interface, the electronic coupling between molecule and electrode, which is related to the interface connection between the molecule and the electrode

REFERENCES

(1) Xin, N.; Guan, J.; Zhou, C.; Chen, X.; Gu, C.; Li, Y.; Ratner, M. A.; Nitzan, A.; Stoddart, J. F.; Guo, X. Concepts in the Design and Engineering of Single-Molecule Electronic Devices. *Nat. Rev. Phys.* **2019**, *1*, 211−230.

(2) Su, T. A.; Neupane, M.; Steigerwald, M. L.; Venkataraman, L.; Nuckolls, C. Chemical Principles of Single-Molecule Electronics. *Nat. Rev. Mater.* **2016**, *1*, 16002.

(3) Sun, L.; Diaz-Fernandez, Y. A.; Gschneidtner, T. A.; Westerlund, F.; Lara-Avila, S.; Moth-Poulsen, K. Single-molecule Electronics: From Chemical Design to Functional Devices. *Chem. Soc. Rev.* **2014**, *43*, 7378−7411.

(4) Qiu, K.; Fato, T. P.; Yuan, B.; Long, Y. T. Toward Precision Measurement and Manipulation of Single-Molecule Reactions by a Confined Space. *Small* **2019**, *15*, No. 1805426.

(5) Liu, J.; Huang, X.; Wang, F.; Hong, W. Quantum Interference Effects in Charge Transport through Single-Molecule Junctions: Detection, Manipulation, and Application. *Acc. Chem. Res.* **2019**, *52*, 151−160.

(6) Gehring, P.; Thijssen, J. M.; van der Zant, H. S. J. Single-Molecule Quantum-Transport Phenomena in Break Junctions. *Nat. Rev. Phys.* **2019**, *1*, 381−396.

(7) Nichols, R. J.; Higgins, S. J. Single Molecule Nanoelectrochemistry in Electrical Junctions. *Acc. Chem. Res.* **2016**, *49*, 2640−2648.

(8) Selzer, Y.; Allara, D. L. Single-Molecule Electrical Junctions. *Annu. Rev. Phys. Chem.* **2006**, *57*, 593−623.

(9) Frisenda, R.; Stefani, D.; van der Zant, H. S. J. Quantum Transport through a Single Conjugated Rigid Molecule, a Mechanical Break Junction Study. *Acc. Chem. Res.* **2018**, *51*, 1359−1367.

(10) Fu, B.; Mosquera, M. A.; Schatz, G. C.; Ratner, M. A.; Hsu, L. Y. Photoinduced Anomalous Coulomb Blockade and the Role of Triplet States in Electron Transport through an Irradiated Molecular Transistor. *Nano Lett.* **2018**, *18*, 5015−5023.

(11) Park, J.; Pasupathy, A. N.; Goldsmith, J. I.; Chang, C.; Yaish, Y.; Petta, J. R.; Rinkoski, M.; Sethna, J. P.; Abruna, H. D.; McEuen, P. L.; Ralph, D. C. Coulomb Blockade and the Kondo Effect in Single-Atom Transistors. *Nature* **2002**, *417*, 722−725.

(12) Manso, M.; Koole, M.; Mulder, M.; Olavarria-Contreras, I. J.; Andersen, C. L.; Jevric, M.; Broman, S. L.; Kadziola, A.; Hammerich, O.; van der Zant, H. S. J.; Nielsen, M. B. Synthesis and Single-Molecule Conductances of Neutral and Cationic Indenofluorene-Extended Tetrathiafulvalenes: Kondo Effect Molecules. *J. Org. Chem.* **2016**, *81*, 8406−8414.

(13) Zhang, L.; Bagrets, A.; Xenioti, D.; Korytar, R.; Schackert, M.; Miyamachi, T.; Schramm, F.; Fuhr, O.; Chandrasekar, R.; Alouani, M.; Ruben, M.; Wulfhekel, W.; Evers, F. Kondo Effect in Binuclear Metal-Organic Complexes with Weakly Interacting Spins. *Phys. Rev. B* **2015**, *91*, 195424.

(14) Frisenda, R.; Gaudenzi, R.; Franco, C.; Mas-Torrent, M.; Rovira, C.; Veciana, J.; Alcon, I.; Bromley, S. T.; Burzuri, E.; van der Zant, H. S. J. Kondo Effect in a Neutral and Stable All Organic Radical Single Molecule Break Junction. *Nano Lett.* **2015**, *15*, 3109−3114.

(15) Parks, J. J.; Champagne, A. R.; Costi, T. A.; Shum, W. W.; Pasupathy, A. N.; Neuscamman, E.; Flores-Torres, S.; Cornaglia, P. S.; Aligia, A. A.; Balseiro, C. A.; Chan, G. K. L.; Abruna, H. D.; Ralph, D. C. Mechanical Control of Spin States in Spin-1 Molecules and the Underscreened Kondo Effect. *Science* **2010**, *328*, 1370−1373.

(16) Ke, G.; Duan, C.; Huang, F.; Guo, X. Electrical and Spin Switches in Single-Molecule Junctions. *InfoMater.* **2020**, *2*, 92−112.

(17) Kuang, G.; Zhang, Q.; Lin, T.; Pang, R.; Shi, X.; Xu, H.; Lin, N. Mechanically-Controlled Reversible Spin Crossover of Single Fe-Porphyrin Molecules. *ACS Nano* **2017**, *11*, 6295−6300.

(18) Aravena, D.; Ruiz, E. Coherent Transport Through Spin-Crossover Single Molecules. *J. Am. Chem. Soc.* **2012**, *134*, 777−779.

(19) Xin, N.; Wang, J.; Jia, C.; Liu, Z.; Zhang, X.; Yu, C.; Li, M.; Wang, S.; Gong, Y.; Sun, H.; Zhang, G.; Liu, Z.; Zhang, G.; Liao, J.; Zhang, D.; Guo, X. Stereoelectronic Effect-Induced Conductance Switching in Aromatic Chain Single-Molecule Junctions. *Nano Lett.* **2017**, *17*, 856−861.

(20) Meng, L.; Xin, N.; Wang, J.; Xu, J.; Ren, S.; Yan, Z.; Zhang, M.; Shen, C.; Zhang, G.; Guo, X.; Meng, S. Atomically Precise Engineering of Single-Molecule Stereoelectronic Effect. *Angew. Chem., Int. Ed.* **2021**, *60*, 12274−12278.

(21) Yao, R. X.; Li, X.; Xiao, N.; Weng, W. G.; Zhang, W. K. Single-Molecule Observation of Mechanical Isomerization of Spirothiopyran and Subsequent Click Addition. *Nano Res.* **2021**, *14*, 2654−2658.

(22) Tamaki, T.; Minode, K.; Numai, Y.; Ohto, T.; Yamada, R.; Masai, H.; Tada, H.; Terao, J. Mechanical Switching of Current-Voltage Characteristics in Spiropyran Single-Molecule Junctions. *Nanoscale* **2020**, *12*, 7527−7531.

(23) Gu, C.; Hu, C.; Wei, Y.; Lin, D.; Jia, C.; Li, M.; Su, D.; Guan, J.; Xia, A.; Xie, L.; Nitzan, A.; Guo, H.; Guo, X. Label-Free Dynamic Detection of Single-Molecule Nucleophilic-Substitution Reactions. *Nano Lett.* **2018**, *18*, 4156−4162.

(24) Guan, J. X.; Jia, C. C.; Li, Y. W.; Liu, Z. T.; Wang, J. Y.; Yang, Z. Y.; Gu, C. H.; Su, D. K.; Houk, K. N.; Zhang, D. Q.; Guo, X. F. Direct Single-Molecule Dynamic Detection of Chemical Reactions. *Sci. Adv.* **2018**, *4*, No. eaar2177.

(25) Aragones, A. C.; Haworth, N. L.; Darwish, N.; Ciampi, S.; Bloomfield, N. J.; Wallace, G. G.; Diez-Perez, I.; Coote, M. L. Electrostatic Catalysis of a Diels-Alder Reaction. *Nature* **2016**, *531*, 88−91.

(26) Yang, C.; Liu, Z. T.; Li, Y. W.; Zhou, S. Y.; Lu, C. X.; Guo, Y. L.; Ramirez, M.; Zhang, Q. Z.; Li, Y.; Liu, Z. R.; Houk, K. N.; Zhang, D. Q.; Guo, X. F. Electric Field-catalyzed Single-Molecule Diels-Alder Reaction Dynamics. *Sci. Adv.* **2021**, *7*, No. eabf0689.

(27) Yang, C.; Zhang, L.; Lu, C.; Zhou, S.; Li, X.; Li, Y.; Yang, Y.; Li, Y.; Liu, Z.; Yang, J.; Houk, K. N.; Mo, F.; Guo, X. Unveiling the Full Reaction Path of the Suzuki-Miyaura Cross-Coupling in a Single-Molecule Junction. *Nat. Nanotechnol.* **2021**, *16*, 1214−1223.

(28) Li, Y.; Zhao, L.; Yao, Y.; Guo, X. Single-Molecule Nanotechnologies: An Evolution in Biological Dynamics Detection. *ACS Appl. Bio. Mater.* **2020**, *3*, 68−85.

(29) Zhuang, X. W.; Bartley, L. E.; Babcock, H. P.; Russell, R.; Ha, T. J.; Herschlag, D.; Chu, S. A Single-Molecule Study of RNA Catalysis and Folding. *Science* **2000**, *288*, 2048−2051.

(30) Wang, J.; Wang, Q.; Zhang, M. Development and Prospect of Near-field Optical Measurements and Characterizations. *Front. Opto.* **2012**, *5*, 171−181.

(31) Halpern, A. R.; Wood, J. B.; Wang, Y.; Corn, R. M. Single-Nanoparticle Near-Infrared Surface Plasmon Resonance Microscopy for Real-Time Measurements of DNA Hybridization Adsorption. *ACS Nano* **2014**, *8*, 1022−1030.

(32) Neuman, K. C.; Nagy, A. Single-Molecule Force Spectroscopy: Optical Tweezers, Magnetic Tweezers and Atomic Force Microscopy. *Nat. Methods.* **2008**, *5*, 491−505.

(33) Zhu, Y.; Tan, Z.; Hong, W. Simultaneous Electrical and Mechanical Characterization of Single-Molecule Junctions Using AFM-BJ Technique. *ACS Omega* **2021**, *6*, 30873−30888.

(34) Xiang, D.; Wang, X.; Jia, C.; Lee, T.; Guo, X. Molecular-Scale Electronics: From Concept to Function. *Chem. Rev.* **2016**, *116*, 4318−4440.

https://doi.org/10.1021/acsnano.1c11433
ACS Nano XXXX, XXX, XXX−XXX

(35) Dekker, C. Solid-State Nanopores. *Nat. Nanotechnol.* **2007**, *2*, 209−215.
(36) Guo, X. Molecular Electronics: Challenges and Opportunities. *AIMS Mater. Sci.* **2014**, *1*, 11−14.
(37) Nitzan, A.; Ratner, M. A. Electron Transport in Molecular Wire Junctions. *Science* **2003**, *300*, 1384−1389.
(38) Guo, X. Molecular Engineering: A Key Route to Improve the Performance of Molecular Devices. *Matter* **2020**, *2*, 284−285.
(39) Aradhya, S. V.; Venkataraman, L. Single-Molecule Junctions Beyond Electronic Transport. *Nat. Nanotechnol.* **2013**, *8*, 399−410.
(40) Isshiki, Y.; Matsuzawa, Y.; Fujii, S.; Kiguchi, M. Investigation on Single-Molecule Junctions Based on Current(−)Voltage Characteristics. *Micromachines* **2018**, *9*, 67.
(41) Li, Y.; Yang, C.; Guo, X. Single-Molecule Electrical Detection: A Promising Route toward the Fundamental Limits of Chemistry and Life Science. *Acc. Chem. Res.* **2020**, *53*, 159−169.
(42) Su, D.; Gu, C.; Guo, X. Functional Molecular Electronic Devices Through Environmental Control. *Sci. China Mater.* **2019**, *62*, 1−7.
(43) Yu, P.; Feng, A.; Zhao, S.; Wei, J.; Yang, Y.; Shi, J.; Hong, W. Recent Progress of Break Junction Technique in Single-Molecule Reaction Chemistry. *Acta. Physico-Chimica. Sinica.* **2019**, *35*, 829−839.
(44) Yang, C.; Qin, A.; Tang, B. Z.; Guo, X. Fabrication and Functions of Graphene-Molecule-Graphene Single-Molecule Junctions. *J. Chem. Phys.* **2020**, *152*, 120902.
(45) Taniguchi, M.; Tsutsui, M.; Yokota, K.; Kawai, T. Inelastic Electron Tunneling Spectroscopy of Single-Molecule Junctions Using a Mechanically Controllable Break Junction. *Nanotechnology* **2009**, *20*, 434008.
(46) Kim, Y.; Bahoosh, S. G.; Sysoiev, D.; Huhn, T.; Pauly, F.; Scheer, E. Inelastic Electron Tunneling Spectroscopy of Difurylethene-based Photochromic Single-Molecule Junctions. *Beilstein J. Nanotechnol.* **2017**, *8*, 2606−2614.
(47) Pugliese, K. M.; Gul, O. T.; Choi, Y.; Olsen, T. J.; Sims, P. C.; Collins, P. G.; Weiss, G. A. Processive Incorporation of Deoxynucleoside Triphosphate Analogs by Single-Molecule DNA Polymerase I (Klenow Fragment) Nanocircuits. *J. Am. Chem. Soc.* **2015**, *137*, 9587−9594.
(48) Choi, Y.; Olsen, T. J.; Sims, P. C.; Moody, I. S.; Corso, B. L.; Dang, M. N.; Weiss, G. A.; Collins, P. G. Dissecting Single-Molecule Signal Transduction in Carbon Nanotube Circuits with Protein Engineering. *Nano Lett.* **2013**, *13*, 625−631.
(49) Jia, C.; Guo, X. Molecule-Electrode Interfaces in Molecular Electronic Devices. *Chem. Soc. Rev.* **2013**, *42*, 5642−5660.
(50) Moth-Poulsen, K.; Bjornholm, T. Molecular Electronics with Single Molecules in Solid-State Devices. *Nat. Nanotechnol.* **2009**, *4*, 551−556.
(51) Song, H.; Kim, Y.; Jang, Y. H.; Jeong, H.; Reed, M. A.; Lee, T. bservation of Molecular Orbital Gating. *Nature* **2009**, *462*, 1039−1043.
(52) Danilov, A.; Kubatkin, S.; Kafanov, S.; Hedegard, P.; Stuhr-Hansen, N.; Moth-Poulsen, K.; Bjornholm, T. Electronic Transport in Single Molecule Junctions: Control of the Molecule-Electrode Coupling Through Intramolecular Tunneling Barriers. *Nano Lett.* **2008**, *8*, 1−5.
(53) Xu, Q.; Scuri, G.; Mathewson, C.; Kim, P.; Nuckolls, C.; Bouilly, D. Single Electron Transistor with Single Aromatic Ring Molecule Covalently Connected to Graphene Nanogaps. *Nano Lett.* **2017**, *17*, 5335−5341.
(54) Mol, J. A.; Lau, C. S.; Lewis, W. J.; Sadeghi, H.; Roche, C.; Cnossen, A.; Warner, J. H.; Lambert, C. J.; Anderson, H. L.; Briggs, G. A. Graphene-Porphyrin Single-Molecule Transistors. *Nanoscale* **2015**, *7*, 13181−13185.
(55) Kubatkin, S.; Danilov, A.; Hjort, M.; Cornil, J.; Bredas, J. L.; Stuhr-Hansen, N.; Hedegard, P.; Bjornholm, T. Single-Electron Transistor of a Single Organic Molecule with Access to Several Redox States. *Nature* **2003**, *425*, 698−701.
(56) Xin, N.; Li, X.; Jia, C.; Gong, Y.; Li, M.; Wang, S.; Zhang, G.; Yang, J.; Guo, X. Tuning Charge Transport in Aromatic-Ring Single-Molecule Junctions via Ionic-Liquid Gating. *Angew. Chem., Int. Ed.* **2018**, *57*, 14026−14031.
(57) Xin, N.; Kong, X.; Zhang, Y. P.; Jia, C.; Liu, L.; Gong, Y.; Zhang, W.; Wang, S.; Zhang, G.; Zhang, H. L.; Guo, H.; Guo, X. Control of Unipolar/Ambipolar Transport in Single-Molecule Transistors through Interface Engineering. *Adv. Electro. Mater.* **2020**, *6*, 1901237.
(58) Zhang, J. D.; Kuznetsov, A. M.; Medvedev, I. G.; Chi, Q. J.; Albrecht, T.; Jensen, P. S.; Ulstrup, J. Single-Molecule Electron Transfer in Electrochemical Environments. *Chem. Rev.* **2008**, *108*, 2737−2791.
(59) Bai, J.; Li, X.; Zhu, Z.; Zheng, Y.; Hong, W. Single-Molecule Electrochemical Transistors. *Adv. Mater.* **2021**, *33*, No. 2005883.
(60) Dickinson, E. J. F.; Wain, A. J. The Butler-Volmer Equation in Electrochemical Theory: Origins, Value, and Practical Application. *J. Electroanal. Chem.* **2020**, *872*, 114145.
(61) Wang, Y. H.; Yan, F.; Li, D. F.; Xi, Y. F.; Cao, R.; Zheng, J. F.; Shao, Y.; Jin, S.; Chen, J. Z.; Zhou, X. S. Enhanced Gating Performance of Single-Molecule Conductance by Heterocyclic Molecules. *J. Phys. Chem. Lett.* **2021**, *12*, 758−763.
(62) Xu, B. Q.; Xiao, X. Y.; Yang, X. M.; Zang, L.; Tao, N. J. Large Gate Modulation in the Current of a Room Temperature Single Molecule Transistor. *J. Am. Chem. Soc.* **2005**, *127*, 2386−2387.
(63) Li, Y.; Wang, H.; Wang, Z.; Qiao, Y.; Ulstrup, J.; Chen, H. Y.; Zhou, G.; Tao, N. Transition from Stochastic Events to Deterministic Ensemble Average in Electron Transfer Reactions Revealed by Single-Molecule Conductance Measurement. *Proc. Natl. Acad. Sci. U.S.A.* **2019**, *116*, 3407−3412.
(64) Osorio, H. M.; Catarelli, S.; Cea, P.; Gluyas, J. B.; Hartl, F.; Higgins, S. J.; Leary, E.; Low, P. J.; Martin, S.; Nichols, R. J.; Tory, J.; Ulstrup, J.; Vezzoli, A.; Milan, D. C.; Zeng, Q. Electrochemical Single-Molecule Transistors with Optimized Gate Coupling. *J. Am. Chem. Soc.* **2015**, *137*, 14319−14328.
(65) De Haas, W. J.; De Boer, J.; Van Den Berg, G. J. The Electrical Resistance of Gold, Copper and Lead at Low Temperatures. *Physica.* **1934**, *1*, 1115−1124.
(66) Parks, J. J.; Champagne, A. R.; Costi, T. A.; Shum, W. W.; Pasupathy, A. N.; Neuscamman, E.; Flores-Torres, S.; Cornaglia, P. S.; Aligia, A. A.; Balseiro, C. A.; Chan, G. K.; Abruna, H. D.; Ralph, D. C. Mechanical Control of Spin States in Spin-1 Molecules and the Underscreened Kondo Effect. *Science* **2010**, *328*, 1370−1373.
(67) Scott, G. D.; Natelson, D. Kondo Resonances in Molecular Devices. *ACS Nano* **2010**, *4*, 3560−3579.
(68) Ruiz, E. Charge Transport Properties of Spin Crossover Systems. *Phys. Chem. Chem. Phys.* **2014**, *16*, 14−22.
(69) Requist, R.; Baruselli, P. P.; Smogunov, A.; Fabrizio, M.; Modesti, S.; Tosatti, E. Magnetic and Molecular Nanocontacts. *Nat. Nanotechnol.* **2016**, *11*, 499−508.
(70) Liang, W. J.; Shores, M. P.; Bockrath, M.; Long, J. R.; Park, H. Kondo Resonance in a Single-Molecule Transistor. *Nature* **2002**, *417*, 725−729.
(71) Scott, G. D.; Hu, T. C. Gate-Controlled Kondo effect in a Single-Molecule Transistor with Elliptical Ferromagnetic Leads. *Phys. Rev. B* **2017**, *96*, 144416.
(72) Brooker, S. Spin Crossover with Thermal Hysteresis: Practicalities and Lessons Learnt. *Chem. Soc. Rev.* **2015**, *44*, 2880−2892.
(73) Molnar, G.; Rat, S.; Salmon, L.; Nicolazzi, W.; Bousseksou, A. Spin Crossover Nanomaterials: From Fundamental Concepts to Devices. *Adv. Mater.* **2018**, *30*, 1703862.
(74) Baadji, N.; Sanvito, S. Giant Resistance Change Across the Phase Transition in Spin-Crossover Molecules. *Phys. Rev. Lett.* **2012**, *108*, 217201.
(75) Frisenda, R.; Harzmann, G. D.; Celis Gil, J. A.; Thijssen, J. M.; Mayor, M.; van der Zant, H. S. Stretching-Induced Conductance Increase in a Spin-Crossover Molecule. *Nano Lett.* **2016**, *16*, 4733−4737.

https://doi.org/10.1021/acsnano.1c11433
ACS Nano XXXX, XXX, XXX−XXX

(76) Harzmann, G. D.; Frisenda, R.; van der Zant, H. S.; Mayor, M. Single-Molecule Spin Switch Based on Voltage-Triggered Distortion of the Coordination Sphere. *Angew. Chem., Int. Ed.* **2015**, *54*, 13425−13430.
(77) Osorio, E. A.; Moth-Poulsen, K.; van der Zant, H. S.; Paaske, J.; Hedegard, P.; Flensberg, K.; Bendix, J.; Bjornholm, T. Electrical Manipulation of Spin States in a Single Electrostatically Gated Transition-metal Complex. *Nano Lett.* **2010**, *10*, 105−110.
(78) Burzuri, E.; Garcia-Fuente, A.; Garcia-Suarez, V.; Senthil Kumar, K.; Ruben, M.; Ferrer, J.; van der Zant, H. S. J. Spin-State Dependent Conductance Switching in Single Molecule-Graphene Junctions. *Nanoscale* **2018**, *10*, 7905−7911.
(79) Baadji, N.; Piacenza, M.; Tugsuz, T.; Della Sala, F.; Maruccio, G.; Sanvito, S. Electrostatic Spin Crossover Effect in Polar Magnetic Molecules. *Nat. Mater.* **2009**, *8*, 813−817.
(80) Wagner, S.; Kisslinger, F.; Ballmann, S.; Schramm, F.; Chandrasekar, R.; Bodenstein, T.; Fuhr, O.; Secker, D.; Fink, K.; Ruben, M.; Weber, H. B. Switching of A Coupled Spin Pair in A Single-Molecule Junction. *Nat. Nanotechnol.* **2013**, *8*, 575−579.
(81) Su, T. A.; Li, H.; Steigerwald, M. L.; Venkataraman, L.; Nuckolls, C. Stereoelectronic Switching in Single-Molecule Junctions. *Nat. Chem.* **2015**, *7*, 215−220.
(82) Tang, Y.; Zhou, Y.; Zhou, D.; Chen, Y.; Xiao, Z.; Shi, J.; Liu, J.; Hong, W. Electric Field-Induced Assembly in Single-Stacking Terphenyl Junctions. *J. Am. Chem. Soc.* **2020**, *142*, 19101−19109.
(83) Seldenthuis, J. S.; Prins, F.; Thijssen, J. M.; van der Zant, H. S. J. An All-Electric Single-Molecule Motor. *ACS Nano* **2010**, *4*, 6681−6686.
(84) Chen, L.; Feng, A.; Wang, M.; Liu, J.; Hong, W.; Guo, X.; Xiang, D. Towards Single-Molecule Optoelectronic Devices. *Sci. China Chem.* **2018**, *61*, 1368−1384.
(85) Liu, W.; Yang, S.; Li, J.; Su, G.; Ren, J. C. One molecule, two states: Single Molecular Switch on Metallic Electrodes. *WIREs Comput. Mol. Sci.* **2021**, *11*, No. e1511.
(86) Shi, C. Y.; Zhang, Q.; Tian, H.; Qu, D. H. Supramolecular Adhesive Materials from Small-Molecule Self-Assembly. *SmartMat* **2020**, *1*, No. e1012.
(87) Tian, H.; Yang, S. Recent Progresses on Diarylethene Based Photochromic Switches. *Chem. Soc. Rev.* **2004**, *33*, 85−97.
(88) Tam, E. S.; Parks, J. J.; Shum, W. W.; Zhong, Y. W.; Santiago-Berrios, M. B.; Zheng, X.; Yang, W. T.; Chan, G. K. L.; Abruna, H. D.; Ralph, D. C. Single-Molecule Conductance of Pyridine-Terminated Dithienylethene Switch Molecules. *ACS Nano* **2011**, *5*, 5115−5123.
(89) Dulic, D.; van der Molen, S. J.; Kudernac, T.; Jonkman, H. T.; de Jong, J. J. D.; Bowden, T. N.; van Esch, J.; Feringa, B. L.; van Wees, B. J. One-Way Optoelectronic Switching of Photochromic Molecules on Gold. *Phys. Rev. Lett.* **2003**, *91*, 207402.
(90) Whalley, A. C.; Steigerwald, M. L.; Guo, X.; Nuckolls, C. Reversible Switching in Molecular Electronic Devices. *J. Am. Chem. Soc.* **2007**, *129*, 12590−12591.
(91) Jia, C.; Wang, J.; Yao, C.; Cao, Y.; Zhong, Y.; Liu, Z.; Liu, Z.; Guo, X. Conductance Switching and Mechanisms in Single-Molecule Junctions. *Angew. Chem., Int. Ed.* **2013**, *52*, 8666−8670.
(92) Jia, C. C.; Migliore, A.; Xin, N.; Huang, S. Y.; Wang, J. Y.; Yang, Q.; Wang, S. P.; Chen, H. L.; Wang, D. M.; Feng, B. Y.; Liu, Z. R.; Zhang, G. Y.; Qu, D. H.; Tian, H.; Ratner, M. A.; Xu, H. Q.; Nitzan, A.; Guo, X. F. Covalently Bonded Single-Molecule Junctions with Stable and Reversible Photoswitched Conductivity. *Science* **2016**, *352*, 1443−1445.
(93) Xin, N.; Jia, C.; Wang, J.; Wang, S.; Li, M.; Gong, Y.; Zhang, G.; Zhu, D.; Guo, X. Thermally Activated Tunneling Transition in a Photoswitchable Single-Molecule Electrical Junction. *J. Phys. Chem. Lett.* **2017**, *8*, 2849−2854.
(94) Bleger, D.; Hecht, S. Visible-Light-Activated Molecular Switches. *Angew. Chem., Int. Ed.* **2015**, *54*, 11338−11349.
(95) Bandara, H. M.; Burdette, S. C. Photoisomerization in Different Classes of Azobenzene. *Chem. Soc. Rev.* **2012**, *41*, 1809−1825.
(96) Cao, Y.; Dong, S.; Liu, S.; Liu, Z.; Guo, X. Toward Functional Molecular Devices based on Graphene-Molecule Junctions. *Angew. Chem., Int. Ed.* **2013**, *52*, 3906−3910.
(97) Chen, X.; Yeoh, Y. Q.; He, Y.; Zhou, C.; Horsley, J. R.; Abell, A. D.; Yu, J.; Guo, X. Unravelling Structural Dynamics within a Photoswitchable Single Peptide: A Step Towards Multimodal Bioinspired Nanodevices. *Angew. Chem., Int. Ed.* **2020**, *59*, 22554−22562.
(98) Meng, L.; Xin, N.; Hu, C.; Wang, J.; Gui, B.; Shi, J.; Wang, C.; Shen, C.; Zhang, G.; Guo, H.; Meng, S.; Guo, X. Side-Group Chemical Gating via Reversible Optical and Electric Control in A Single Molecule Transistor. *Nat. Commun.* **2019**, *10*, 1450.
(99) Roldan, D.; Kaliginedi, V.; Cobo, S.; Kolivoska, V.; Bucher, C.; Hong, W.; Royal, G.; Wandlowski, T. Charge Transport in Photoswitchable Dimethyldihydropyrene-Type Single-Molecule Junctions. *J. Am. Chem. Soc.* **2013**, *135*, 5974−5977.
(100) Huang, C.; Jevric, M.; Borges, A.; Olsen, S. T.; Hamill, J. M.; Zheng, J. T.; Yang, Y.; Rudnev, A.; Baghernejad, M.; Broekmann, P.; Petersen, A. U.; Wandlowski, T.; Mikkelsen, K. V.; Solomon, G. C.; Brondsted Nielsen, M.; Hong, W. Single-Molecule Detection of Dihydroazulene Photo-thermal Reaction Using Break Junction Technique. *Nat. Commun.* **2017**, *8*, 15436.
(101) Darwish, N.; Aragones, A. C.; Darwish, T.; Ciampi, S.; Diez-Perez, I. Multi-Responsive Photo- and Chemo-electrical Single-Molecule Switches. *Nano Lett.* **2014**, *14*, 7064−7070.
(102) Wang, Z.; Ma, Z.; Wang, Y.; Xu, Z.; Luo, Y.; Wei, Y.; Jia, X. A Novel Mechanochromic and Photochromic Polymer Film: When Rhodamine Joins Polyurethane. *Adv. Mater.* **2015**, *27*, 6469−6474.
(103) Raisch, M.; Maftuhin, W.; Walter, M.; Sommer, M. A Mechanochromic Donor-Acceptor Torsional Spring. *Nat. Commun.* **2021**, *12*, 4243.
(104) Jung, S.; Yoon, H. J. Mechanical Force for the Transformation of Aziridine into Imine. *Angew. Chem., Int. Ed.* **2021**, *60*, 23564−23568.
(105) Cha, Y.; Zhu, T.; Sha, Y.; Lin, H.; Hwang, J.; Seraydarian, M.; Craig, S. L.; Tang, C. Mechanochemistry of Cationic Cobaltocenium Mechanophore. *J. Am. Chem. Soc.* **2021**, *143*, 11871−11878.
(106) Ramirez, A. L.; Kean, Z. S.; Orlicki, J. A.; Champhekar, M.; Elsakr, S. M.; Krause, W. E.; Craig, S. L. Mechanochemical Strengthening of A Synthetic Polymer in Response to Typically Destructive Shear Forces. *Nat. Chem.* **2013**, *5*, 757−761.
(107) Zhao, H.; Huang, L.; Wang, Y.; Feng, K.; Chang, Y.; Huang, S.; Ma, C.; Yan, X. Mechanochromic Luminescence of 2,6-Bis(4-biphenyl)isonicotinic Acid via Interconversion of Classical/Frustrated Bronsted Pair. *J. Org. Chem.* **2021**, *86*, 12591−12596.
(108) Huang, W.; Zhu, Z.; Wen, J.; Wang, X.; Qin, M.; Cao, Y.; Ma, H.; Wang, W. Single Molecule Study of Force-Induced Rotation of Carbon-Carbon Double Bonds in Polymers. *ACS Nano* **2017**, *11*, 194−203.
(109) Minkin, V. I. Photo-, Thermo-, Solvato-, and Electrochromic Spiroheterocyclic Compounds. *Chem. Rev.* **2004**, *104*, 2751−2776.
(110) Yu, M.; Zhang, P.; Liu, L.; Wang, H.; Wang, H.; Zhang, C.; Gao, Y.; Yang, C.; Cui, J.; Chen, J. Reversibly Photoswitchable Tristate Fluorescence within a Single Polymeric Nanoparticle. *Adv. Opt. Mater.* **2021**, *9*, 2101227.
(111) Dattler, D.; Fuks, G.; Heiser, J.; Moulin, E.; Perrot, A.; Yao, X.; Giuseppone, N. Design of Collective Motions from Synthetic Molecular Switches, Rotors, and Motors. *Chem. Rev.* **2020**, *120*, 310−433.
(112) Walkey, M. C.; Peiris, C. R.; Ciampi, S.; Aragones, A. C.; Dominguez-Espindola, R. B.; Jago, D.; Pulbrook, T.; Skelton, B. W.; Sobolev, A. N.; Diez Perez, I.; Piggott, M. J.; Koutsantonis, G. A.; Darwish, N. Chemically and Mechanically Controlled Single-Molecule Switches Using Spiropyrans. *ACS Appl. Mater. Interfaces* **2019**, *11*, 36886−36894.
(113) Noori, M.; Aragones, A. C.; Di Palma, G.; Darwish, N.; Bailey, S. W.; Al-Galiby, Q.; Grace, I.; Amabilino, D. B.; Gonzalez-Campo, A.; Diez-Perez, I.; Lambert, C. J. Tuning the Electrical Conductance of Metalloporphyrin Supramolecular Wires. *Sci. Rep.* **2016**, *6*, 37352.

https://doi.org/10.1021/acsnano.1c11433
ACS Nano XXXX, XXX, XXX−XXX

(114) Haiss, W.; Wang, C.; Grace, I.; Batsanov, A. S.; Schiffrin, D. J.; Higgins, S. J.; Bryce, M. R.; Lambert, C. J.; Nichols, R. J. Precision Control of Single-Molecule Electrical Junctions. *Nat. Mater.* **2006**, *5*, 995−1002.
(115) Liu, Y.; Wu, S.; Gopalakrishna, T. Y.; Wu, J. Benzo[1,2-c;4,5-c′]bis[1,2,5]Thiadiazole-Porphyrin-Based Near-Infrared Dyes. *SmartMat* **2021**, *2*, 398−405.
(116) Leary, E.; Roche, C.; Jiang, H. W.; Grace, I.; Gonzalez, M. T.; Rubio-Bollinger, G.; Romero-Muniz, C.; Xiong, Y.; Al-Galiby, Q.; Noori, M.; Lebedeva, M. A.; Porfyrakis, K.; Agrait, N.; Hodgson, A.; Higgins, S. J.; Lambert, C. J.; Anderson, H. L.; Nichols, R. J. Detecting Mechanochemical Atropisomerization Within an STM Break Junction. *J. Am. Chem. Soc.* **2018**, *140*, 710−718.
(117) Jensen, F. R.; Noyce, D. S.; Sederholm, C. H.; Berlin, A. J. The Energy Barrier for the Chair-Chair Interconversion of Cyclohexane. *J. Am. Chem. Soc.* **1960**, *82*, 1256−1257.
(118) Tang, C.; Tang, Y.; Ye, Y.; Yan, Z.; Chen, Z.; Chen, L.; Zhang, L.; Liu, J.; Shi, J.; Xia, H.; Hong, W. Identifying the Conformational Isomers of Single-Molecule Cyclohexane at Room Temperature. *Chem.* **2020**, *6*, 2770−2781.
(119) Zang, Y.; Zou, Q.; Fu, T.; Ng, F.; Fowler, B.; Yang, J.; Li, H.; Steigerwald, M. L.; Nuckolls, C.; Venkataraman, L. Directing Isomerization Teactions of Cumulenes with Electric Fields. *Nat. Commun.* **2019**, *10*, 4482.
(120) Quintans, C. S.; Andrienko, D.; Domke, K. F.; Aravena, D.; Koo, S.; Díez-Pérez, I.; Aragonès, A. C. Tuning Single-Molecule Conductance by Controlled Electric Field-Induced *trans*-to-*cis* Isomerisation. *Appl. Sci.* **2021**, *11*, 3317.
(121) Kollman, P. A.; Allen, L. C. The Theory of the Hydrongen Bond. *Chem. Rev.* **1972**, *72*, 283−303.
(122) Grabowski, S. J. What is the Covalency of Hydrogen Bonding? *Chem. Rev.* **2011**, *111*, 2597−2625.
(123) de Rege, P. J.; Williams, S. A.; Therien, M. J. Direct Evaluation of Electronic Coupling Mediated by Hydrogen Bonds: Implications for Biological Electron Transfer. *Science* **1995**, *269*, 1409−1413.
(124) Nishino, T.; Hayashi, N.; Bui, P. T. Direct Measurement of Electron Transfer Through a Hydrogen Bond between Single Molecules. *J. Am. Chem. Soc.* **2013**, *135*, 4592−4595.
(125) Zwolak, M.; Di Ventra, M. Electronic Signature of DNA Nucleotides via Transverse Transport. *Nano Lett.* **2005**, *5*, 421−424.
(126) Chang, S.; He, J.; Kibel, A.; Lee, M.; Sankey, O.; Zhang, P.; Lindsay, S. Tunnelling Readout of Hydrogen-Bonding-Based Recognition. *Nat. Nanotechnol.* **2009**, *4*, 297−301.
(127) Huang, S.; He, J.; Chang, S.; Zhang, P.; Liang, F.; Li, S.; Tuchband, M.; Fuhrmann, A.; Ros, R.; Lindsay, S. Identifying Single Bases in a DNA Oligomer with Electron Tunnelling. *Nat. Nanotechnol.* **2010**, *5*, 868−873.
(128) Zhou, C.; Li, X.; Gong, Z.; Jia, C.; Lin, Y.; Gu, C.; He, G.; Zhong, Y.; Yang, J.; Guo, X. Direct Observation of Single-Molecule Hydrogen-Bond Dynamics with Single-Bond Resolution. *Nat. Commun.* **2018**, *9*, 807.
(129) Beijer, F. H.; Sijbesma, R. P.; Kooijman, H.; Spek, A. L.; Meijer, E. W. Strong Dimerization of Ureidopyrimidones via Quadruple Hydrogen Bonding. *J. Am. Chem. Soc.* **1998**, *120*, 6761−6769.
(130) Hu, Q. D.; Tang, G. P.; Chu, P. K. Cyclodextrin-Based Host-Guest Supramolecular Nanoparticles for Delivery: From Design to Applications. *Acc. Chem. Res.* **2014**, *47*, 2017−2025.
(131) Wankar, J.; Kotla, N. G.; Gera, S.; Rasala, S.; Pandit, A.; Rochev, Y. A. Recent Advances in Host−Guest Self-Assembled Cyclodextrin Carriers: Implications for Responsive Drug Delivery and Biomedical Engineering. *Adv. Funct. Mater.* **2020**, *30*, 1909049.
(132) Ma, X.; Zhao, Y. Biomedical Applications of Supramolecular Systems Based on Host-Guest Interactions. *Chem. Rev.* **2015**, *115*, 7794−7839.
(133) Chen, H.; Fraser Stoddart, J. From Molecular to Supramolecular Electronics. *Nat. Rev. Mater.* **2021**, *6*, 804−828.
(134) Lee, J. W.; Samal, S.; Selvapalam, N.; Kim, H. J.; Kim, K. C Cucurbituril Homologues and Derivatives: New Opportunities in Supramolecular Chemistry. *Acc. Chem. Res.* **2003**, *36*, 621−630.
(135) Ni, X. L.; Xiao, X.; Cong, H.; Zhu, Q. J.; Xue, S. F.; Tao, Z. Self-Assemblies Based on the "Outer-Surface Interactions" of Cucurbit[n]urils: New Opportunities for Supramolecular Architectures and Materials. *Acc. Chem. Res.* **2014**, *47*, 1386−1395.
(136) Kawaguchi, Y.; Harada, A. An Electric Trap: A New Method for Entrapping Cyclodextrin in A Rotaxane Structure. *J. Am. Chem. Soc.* **2000**, *122*, 3797−3798.
(137) Jeon, W. S.; Kim, E.; Ko, Y. H.; Hwang, I.; Lee, J. W.; Kim, S.-Y.; Kim, H.-J.; Kim, K. Molecular Loop Lock: A Redox-Driven Molecular Machine Based on a Host-Stabilized Charge-Transfer Complex. *Angew. Chem., Int. Ed.* **2005**, *117*, 89−93.
(138) Biedermann, F.; Vendruscolo, M.; Scherman, O. A.; De Simone, A.; Nau, W. M. Cucurbit[8]uril and Blue-Box: High-Energy water release overwhelms electrostatic interactions. *J. Am. Chem. Soc.* **2013**, *135*, 14879−14888.
(139) Zhang, W.; Gan, S.; Vezzoli, A.; Davidson, R. J.; Milan, D. C.; Luzyanin, K. V.; Higgins, S. J.; Nichols, R. J.; Beeby, A.; Low, P. J.; Li, B.; Niu, L. Single-Molecule Conductance of Viologen-Cucurbit[8]uril Host-Guest Complexes. *ACS Nano* **2016**, *10*, 5212−5220.
(140) Wen, H. M.; Li, W. G.; Chen, J. W.; He, G.; Li, L. H.; Olson, M. A.; Sue, A. C. H.; Stoddart, J. F.; Guo, X. F. Complex Formation Dynamics in A Single-Molecule Electronic Device. *Sci. Adv.* **2016**, *2*, No. e1601113.
(141) Kiguchi, M.; Nakashima, S.; Tada, T.; Watanabe, S.; Tsuda, S.; Tsuji, Y.; Terao, J. Single-molecule Conductance of π-Conjugated Rotaxane: New Method for Measuring Stipulated Electric Conductance of π-Conjugated Molecular Wire Using STM Break Junction. *Small* **2012**, *8*, 726−730.
(142) Zhou, C.; Li, X.; Masai, H.; Liu, Z.; Lin, Y.; Tamaki, T.; Terao, J.; Yang, J.; Guo, X. Revealing Charge- and Temperature- Dependent Movement Dynamics and Mechanism of Individual Molecular Machines. *Small Methods* **2019**, *3*, 1900464.
(143) Liu, Z. H.; Li, X. X.; Masai, H.; Huang, X. Y.; Tsuda, S.; Terao, J.; Yang, J. L.; Guo, X. F. A Single-Molecule Electrical Approach for Amino Acid Detection and Chirality Recognition. *Sci. Adv.* **2021**, *7*, No. eabe4365.
(144) Muttenthaler, M.; King, G. F.; Adams, D. J.; Alewood, P. F. Trends in Peptide Drug Discovery. *Nat. Rev. Drug. Discovery* **2021**, *20*, 309−325.
(145) Scully, R.; Panday, A.; Elango, R.; Willis, N. A. DNA Double-Strand Break Repair-Pathway Choice in Somatic Mammalian cells. *Nat. Rev. Mol. Cell. Biol.* **2019**, *20*, 698−714.
(146) Fernandez-Leiro, R.; Scheres, S. H. Unravelling Biological Macromolecules with Cryo-electron Microscopy. *Nature* **2016**, *537*, 339−346.
(147) Shen, H.; Li, Z.; Jiang, Y.; Pan, X.; Wu, J.; Cristofori-Armstrong, B.; Smith, J. J.; Chin, Y. K. Y.; Lei, J.; Zhou, Q.; King, G. F.; Yan, N. Structural Basis for the Modulation of Voltage-Gated Sodium Channels by Animal Toxins. *Science* **2018**, *362*, No. eaau2596.
(148) Lipman, E. A.; Schuler, B.; Bakajin, O.; Eaton, W. A. Single-Molecule Measurement of Protein Folding Kinetics. *Science* **2003**, *301*, 1233−1235.
(149) Chakraborty, A.; Wang, D. Y.; Ebright, Y. W.; Korlann, Y.; Kortkhonjia, E.; Kim, T.; Chowdhury, S.; Wigneshweraraj, S.; Irschik, H.; Jansen, R.; Nixon, B. T.; Knight, J.; Weiss, S.; Ebright, R. H. Opening and Closing of the Bacterial RNA Polymerase Clamp. *Science* **2012**, *337*, 591−595.
(150) Miles, B. N.; Ivanov, A. P.; Wilson, K. A.; Dogan, F.; Japrung, D.; Edel, J. B. Single Molecule Sensing with Solid-State Nanopores: Novel Materials, Methods, and Applications. *Chem. Soc. Rev.* **2013**, *42*, 15−28.
(151) Min, S. K.; Kim, W. Y.; Cho, Y.; Kim, K. S. Fast DNA Sequencing With a Graphene-Based Nanochannel Device. *Nat. Nanotechnol.* **2011**, *6*, 162−165.
(152) Genereux, J. C.; Barton, J. K. Mechanisms for DNA Charge Transport. *Chem. Rev.* **2010**, *110*, 1642−1662.

https://doi.org/10.1021/acsnano.1c11433
ACS Nano XXXX, XXX, XXX−XXX

(153) Wang, K. DNA-Based Single-Molecule Electronics: From Concept to Function. *J. Funct. Biomater.* **2018**, *9*, 8.
(154) Xiang, L.; Palma, J. L.; Li, Y.; Mujica, V.; Ratner, M. A.; Tao, N. Gate-Controlled Conductance Switching in DNA. *Nat. Commun.* **2017**, *8*, 14471.
(155) Wang, X.; Gao, L.; Liang, B.; Li, X.; Guo, X. Revealing the Direct Effect of Individual Intercalations on DNA Conductance Toward Single-Molecule Electrical Biodetection. *J. Mater. Chem. B* **2015**, *3*, 5150−5154.
(156) Chen, X.; Zhou, C.; Guo, X. Ultrasensitive Detection and Binding Mechanism of Cocaine in an Aptamer-Based Single-Molecule Device. *Chin. J. Chem.* **2019**, *37*, 897−902.
(157) Dupont, C. L.; Grass, G.; Rensing, C. Copper Toxicity and the Origin of Bacterial Resistance-New Insights and Applications. *Metallomics.* **2011**, *3*, 1109−1118.
(158) Gao, L.; Li, L. L.; Wang, X.; Wu, P.; Cao, Y.; Liang, B.; Li, X.; Lin, Y.; Lu, Y.; Guo, X. Graphene-DNAzyme Junctions: A Platform for Direct Metal Ion Detection with Ultrahigh Sensitivity. *Chem. Sci.* **2015**, *6*, 2469−2473.
(159) Yi, H.; Zhang, G.; Wang, H.; Huang, Z.; Wang, J.; Singh, A. K.; Lei, A. Recent Advances in Radical C-H Activation/Radical Cross-Coupling. *Chem. Rev.* **2017**, *117*, 9016−9085.
(160) Chen, J. R.; Hu, X. Q.; Lu, L. Q.; Xiao, W. J. Visible Light Photoredox-Controlled Reactions of N-Radicals and Radical Ions. *Chem. Soc. Rev.* **2016**, *45*, 2044−2056.
(161) Ratera, I.; Veciana, J. Playing with Organic Radicals as Building Blocks for Functional Molecular Materials. *Chem. Soc. Rev.* **2012**, *41*, 303−349.
(162) Bergfield, J. P.; Solomon, G. C.; Stafford, C. A.; Ratner, M. A. Novel Quantum Interference Effects in Transport Through Molecular Radicals. *Nano Lett.* **2011**, *11*, 2759−2764.
(163) Karpinska, J.; Starczewska, B.; PuzanowskaTarasiewicz, H. Analytical Properties of 2- and 10-Disubstituted Phenothiazine Derivatives. *Anal. Sci.* **1996**, *12*, 161−170.
(164) Liu, J.; Zhao, X.; Al-Galiby, Q.; Huang, X.; Zheng, J.; Li, R.; Huang, C.; Yang, Y.; Shi, J.; Manrique, D. Z.; Lambert, C. J.; Bryce, M. R.; Hong, W. Radical-Enhanced Charge Transport in Single-Molecule Phenothiazine Electrical Junctions. *Angew. Chem., Int. Ed.* **2017**, *56*, 13061−13065.
(165) Yang, G.; Sangtarash, S.; Liu, Z.; Li, X.; Sadeghi, H.; Tan, Z.; Li, R.; Zheng, J.; Dong, X.; Liu, J.; Yang, Y.; Shi, J.; Xiao, Z.; Zhang, G.; Lambert, C.; Hong, W.; Zhang, D. Protonation Tuning of Quantum Interference in Azulene-Type Single-Molecule Junctions. *Chem. Sci.* **2017**, *8*, 7505−7509.
(166) Yang, C.; Zhang, L.; Li, H.; Guo, Y.; Jia, C.; Zhu, W.; Mo, F.; Guo, X. Single-molecule Electrical Spectroscopy of Organocatalysis. *Matter* **2021**, *4*, 2874−2885.
(167) Praetorius, J. M.; Crudden, C. M. N-Heterocyclic Carbene Complexes of Rhodium: Structure, Stability and Reactivity. *Dalton. Trans.* **2008**, 4079−4094.
(168) Ciampi, S.; Darwish, N.; Aitken, H. M.; Diez-Perez, I.; Coote, M. L. Harnessing Electrostatic Catalysis in Single Molecule, Electrochemical and Chemical Systems: A Rapidly Growing Experimental Tool Box. *Chem. Soc. Rev.* **2018**, *47*, 5146−5164.
(169) Shaik, S.; Ramanan, R.; Danovich, D.; Mandal, D. Structure and Reactivity/Selectivity Control by Oriented-External Electric Fields. *Chem. Soc. Rev.* **2018**, *47*, 5125−5145.
(170) Che, F.; Gray, J. T.; Ha, S.; Kruse, N.; Scott, S. L.; McEwen, J.-S. Elucidating the Roles of Electric Fields in Catalysis: A Perspective. *ACS Catal.* **2018**, *8*, 5153−5174.
(171) Nicolaou, K. C.; Snyder, S. A.; Montagnon, T.; Vassilikogiannakis, G. The Diels-Alder Reaction in Total Synthesis. *Angew. Chem., Int. Ed.* **2002**, *41*, 1668−1698.
(172) Nawrat, C. C.; Moody, C. J. Quinones as Dienophiles in the Diels-Alder reaction: History and Applications in Total Synthesis. *Angew. Chem., Int. Ed.* **2014**, *53*, 2056−2077.
(173) Meir, R.; Chen, H.; Lai, W.; Shaik, S. Oriented Electric Fields Accelerate Diels-Alder Reactions and Control the Endo/Exo Selectivity. *Chemphyschem.* **2010**, *11*, 301−310.
(174) Huang, X. Y.; Tang, C.; Li, J. Q.; Chen, L. C.; Zheng, J. T.; Zhang, P.; Le, J. B.; Li, R. H.; Li, X. H.; Liu, J. Y.; Yang, Y.; Shi, J.; Chen, Z. B.; Bai, M. D.; Zhang, H. L.; Xia, H. P.; Cheng, J.; Tian, Z. Q.; Hong, W. J. Electric Field-Induced Selective Catalysis of Single-Molecule Reaction. *Sci. Adv.* **2019**, *5*, No. eaaw3072.
(175) Somorjai, G. A.; Park, J. Y. Molecular Factors of Catalytic Selectivity. *Angew. Chem., Int. Ed.* **2008**, *47*, 9212−9228.
(176) Zhang, L.; Laborda, E.; Darwish, N.; Noble, B. B.; Tyrell, J. H.; Pluczyk, S.; Le Brun, A. P.; Wallace, G. G.; Gonzalez, J.; Coote, M. L.; Ciampi, S. Electrochemical and Electrostatic Cleavage of Alkoxyamines. *J. Am. Chem. Soc.* **2018**, *140*, 766−774.
(177) Zhang, J. L.; Zhong, J. Q.; Lin, J. D.; Hu, W. P.; Wu, K.; Xu, G. Q.; Wee, A. T.; Chen, W. Towards Single Molecule Switches. *Chem. Soc. Rev.* **2015**, *44*, 2998−3022.
(178) Tsutsui, M.; Taniguchi, M. Single Molecule Electronics and Devices. *Sensors* **2012**, *12*, 7259−7298.

https://doi.org/10.1021/acsnano.1c11433
ACS Nano XXXX, XXX, XXX−XXX